

Journal of Visualized Experiments

Contrast-Matching Detergent in Small-Angle Neutron Scattering Experiments for Membrane Protein Structural Analysis and Ab Initio Modeling --Manuscript Draft--

Article Type:	Invited Methods Article - JoVE Produced Video
Manuscript Number:	JoVE57901R2
Full Title:	Contrast-Matching Detergent in Small-Angle Neutron Scattering Experiments for Membrane Protein Structural Analysis and Ab Initio Modeling
Keywords:	Small Angle Scattering; Neutron Scattering; biophysics; membrane protein; Contrast Variation; Surfactant; Micelle; Intramembrane Aspartyl Protease; Presenilin; Signal Peptide Peptidase
Corresponding Author:	Volker S Urban Oak Ridge National Laboratory Oak Ridge, Tennessee UNITED STATES
Corresponding Author's Institution:	Oak Ridge National Laboratory
Corresponding Author E-Mail:	urbanvs@ornl.gov
First Author:	Ryan Oliver
Other Authors:	Ryan Oliver
	Swe-Htet Naing
	Kevin L Weiss
	Sai Venkatesh Pingali
	Raquel L Lieberman
Author Comments:	
Additional Information:	
Question	Response
If this article needs to be "in-press" by a certain date, please indicate the date below and explain in your cover letter.	

January 22, 2018

To:
Jialan Zhang, Ph.D.
Science Editor
JoVE

Dear Dr. Zhang,

Following your invitation, we are submitting the manuscript “Contrast-Matching Detergent in Small-Angle Neutron Scattering Experiments for Membrane Protein Structural Analysis and *Ab Initio* Modeling” for publication in *JoVE*. The presented methods are uniquely capable of determining solution structures of intrinsic membrane proteins by eliminating any measurement signal perturbations from associated detergent molecules. The methods are generally applicable for studying membrane proteins and interactions between such proteins and their binding partners or substrates etc. The specific example in this protocol demonstrates how to obtain a low-resolution *ab initio* model and structural details of a detergent-solubilized membrane protein—MmIAP, an intramembrane aspartyl protease from *Methanoculleus marisnigri*—in solution using small-angle neutron scattering with contrast-matching of the detergent.

This is a new manuscript, which has not been submitted elsewhere for publication. All coauthors have reviewed the final manuscript and approve its submission to *JoVE*.

Sincerely,



Volker S. Urban, Ph.D.
Neutron Scattering Scientist
Large Scale Structures Group
Neutron Scattering Division
Oak Ridge National Laboratory
PO Box 2008; MS-6475
Oak Ridge, TN 37831
Phone: 865-576-7221
urbanvs@ornl.gov

TITLE:

Contrast-Matching Detergent in Small-Angle Neutron Scattering Experiments for Membrane Protein Structural Analysis and *Ab Initio* Modeling

AUTHORS AND AFFILIATIONS:

Ryan C Oliver¹, Swe-Htet Naing², Kevin L. Weiss¹, Sai Venkatesh Pingali¹, Raquel L. Lieberman², Volker S. Urban¹

¹Neutron Scattering Division, Oak Ridge National Laboratory, Oak Ridge, TN, USA

²School of Chemistry and Biochemistry, Georgia Institute of Technology, Atlanta, GA, USA

Corresponding Author:

Volker S. Urban (urbanvs@ornl.gov)

Tel: (865)-576-7221

Email Addresses of Co-authors:

Ryan C Oliver (oliverrc@ornl.gov)

Swe-Htet Naing (snaing12@gatech.edu)

Kevin L. Weiss (weisskl@ornl.gov)

Sai Venkatesh Pingali (pingalis@ornl.gov)

Raquel L. Lieberman (raquel.lieberman@chemistry.gatech.edu)

KEYWORDS:

Small angle scattering, neutron scattering, biophysics, membrane protein, contrast variation, surfactant, micelle, intramembrane aspartyl protease, presenilin, signal peptide peptidase

SHORT ABSTRACT:

This protocol demonstrates how to obtain a low-resolution *ab initio* model and structural details of a detergent-solubilized membrane protein in solution using small-angle neutron scattering with contrast-matching of the detergent.

LONG ABSTRACT:

The biological small-angle neutron scattering instrument at the High-Flux Isotope Reactor of Oak Ridge National Laboratory is dedicated to the investigation of biological materials, biofuel processing, and bio-inspired materials covering nanometer to micrometer length scales. The methods presented here for investigating physical properties (*i.e.*, size and shape) of membrane proteins (here, MmlAP, an intramembrane aspartyl protease from *Methanoculleus marisnigri*) in solutions of micelle-forming detergents are well-suited for this small-angle neutron scattering instrument, among others. Other biophysical characterization techniques are hindered by their inability to address the detergent contributions in a protein-detergent complex structure. Additionally, access to the Bio-Deuteration Lab provides unique capabilities for preparing large-scale cultivations and expressing deuterium-labeled proteins for enhanced scattering signal from the protein. While this technique does not provide structural details at high-resolution, the structural knowledge gap for membrane proteins contains many addressable areas of research without requiring near-atomic resolution. For example, these areas include determination of

oligomeric states, complex formation, conformational changes during perturbation, and folding/unfolding events. These investigations can be readily accomplished through applications of this method.

INTRODUCTION:

Membrane proteins are encoded by an estimated 30% of all genes¹ and represent a strong majority of targets for modern medicinal drugs². These proteins perform a wide array of vital cellular functions³, but despite their abundance and importance – only represent about 1% of total structures deposited in the Research Collaboratory for Structural Bioinformatics (RCSB) Protein Data Bank⁴. Due to their partially hydrophobic nature, structural determination of membrane-bound proteins has been exceedingly challenging⁵⁻⁷.

As many biophysical techniques require monodisperse particles in solution for measurement, isolating membrane proteins from native membranes and stabilizing these proteins in a soluble mimic of the native membranes has been an active area of research in recent decades⁸⁻¹⁰. These investigations have led to the development of many novel amphiphilic assemblies to solubilize membrane proteins, such as nanodiscs¹¹⁻¹³, bicelles^{14,15}, and amphipols^{16,17}. However, the use of detergent micelles remains one of the most common and straightforward approaches for satisfying the solubility requirements of a given protein¹⁸⁻²⁵. Unfortunately, no single detergent or magic mixture of detergents currently exists that satisfies all membrane proteins; thus, these conditions must be empirically screened for the unique requirements of each protein^{26,27}.

Detergents self-assemble in solution above their critical micelle concentration to form aggregate structures called micelles. Micelles are composed of many detergent monomers (typically ranging from 20-200) with hydrophobic alkyl chains forming a micelle core and hydrophilic head groups arranged in a micelle shell layer facing the aqueous solvent. The behavior of detergents and micelle formation has been classically described by Charles Tanford in *The Hydrophobic Effect*²⁸, and sizes and shapes of micelles from commonly used detergents in membrane protein studies have been characterized using small-angle scattering^{29,30}. Detergent organization about membrane proteins has also been studied, and the formation of protein-detergent complexes (PDCs) is expected with detergent molecules surrounding the protein in an arrangement that resembles the neat detergent micelles³¹.

One added advantage in using detergents is that the resulting micelle properties can be manipulated by incorporating other detergents. Many detergents exhibit ideal mixing, and select properties of mixed micelles may even be predicted from the components and ratio of mixing²². However, the presence of detergent can still present challenges for biophysical characterizations by contributing to the overall signal. For example, with X-ray and light scattering techniques, signal from detergent in the PDC is practically indistinguishable from protein³². Investigations with single-particle cryo-electron microscopy (cryo-EM) typically rely on trapped (frozen) particles; structural details of the protein are still obscured by certain detergents or a high concentration of detergent which adds to the background³³. Alternate approaches toward interpreting the full PDC structure (including the detergent) have been made through computational methods which seek to reconstruct the detergent around a given membrane

protein³⁴.

For the case of neutron scattering, the core-shell arrangement of detergent in the micelle produces a form factor which contributes to the observed scattering. Fortunately, solution components can be altered such that they do not contribute to the net observed scattering. This “contrast matching” process is achieved by substituting deuterium for hydrogen to achieve a scattering length density that matches that of the background (buffer). A judicious choice of detergent (with available deuterated counterparts) and their ratio of mixing must be considered. For detergent micelles, this substitution can be performed using a detergent with the same head group but having a deuterated alkyl chain (d-tail instead of h-tail). Since the detergents are well-mixed³⁵, their aggregates will have a scattering length density that is the mole-fraction weighted average of the two components (h-tails and d-tails). When this average contrast is consistent with that of the head group, the uniform aggregate structures can be fully matched to remove all contributions to observed scattering.

We present here a protocol to manipulate the neutron contrast of detergent micelles by incorporating chemically identical detergent molecules with deuterium-labeled alkyl chains^{19,36,37}. This permits complete simultaneous contrast matching of micelle core and shell, which is a unique capability of neutron scattering^{35,38}. With this significantly refined level of detail, contrast matching can enable otherwise unfeasible studies of membrane protein structures. Additionally, this contrast-matching approach could be extended to other systems involving detergent, such as polymer exchange reactions³⁹ and oil-water dispersants⁴⁰, or even other solubilizing agents, such as bicelles⁴¹, nanodiscs⁴², or block copolymers⁴³. A similar approach as outlined in this manuscript, but employing a single detergent species with partial deuterium substitutions on the alkyl chain and/or head group, was recently published³⁷. While this can be expected to improve the random distribution of hydrogen and deuterium throughout the detergent compared to the approach presented here, the limited number of available positions on the detergent for substitution and two-step detergent synthesis required poses additional challenges for consideration.

Steps 1 and 2 of the protocol detailed below often overlap since initial experiment planning must be done to submit a quality proposal. However, proposal submission is considered here as the first step to emphasize that this process should be started well in advance of a neutron experiment. It should also be noted that a prerequisite step, which should be demonstrated by the proposal, is to have biochemical and physical characterization (including purity and stability) of the sample supporting the need for neutron studies. A general discussion of small-angle neutron scattering (SANS) is beyond the scope of this article. A brief but thorough introduction is available in the reference work *Characterization of Materials* by Kaufmann,⁴⁴ and a comprehensive textbook focused on biological small-angle solution scattering has recently been published.⁴⁵ Further recommended reading is given in the Discussion section. Small angle scattering uses the so called scattering vector Q as the central quantity that describes the scattering process. This article uses the widely accepted definition $Q = 4\pi \sin(\theta)/\lambda$, where θ is half the angle between incoming and scattered beam and λ is the wavelength of the neutron radiation in Angstroms. Other definitions exist that use different symbols such as ‘s’ for the scattering

vector, and that may differ by a factor 2π or by using nanometers in place of Angstrom (see also discussion of **Figure 10**).

PROTOCOL:

1. Prepare and Submit a Neutron Facility Beam Time and Instrument Proposal

1.1. Consult online resources for identifying neutron scattering facilities that provide general user neutron beam time access, such as Oak Ridge National Laboratory (ORNL). A map of neutron facilities and information about neutron research worldwide is available online⁴⁶. Be aware that these facilities typically have regular calls for proposals; this determines when the next beam time will be available. Neutrons are used for a variety of applications; search for small-angle neutron scattering (SANS) instruments, particularly those with capabilities for biological samples.

1.2. Use resources provided by the neutron facilities to help navigate the neutron beam time proposal submission process. Consult with a Neutron Scattering Scientist (NSS) that is associated with the instrument for which you will apply. Review the neutron facility's current information regarding proposal calls, deadlines, and advice for submission; for Oak Ridge this is available online⁴⁷. Submit the beam time proposal following all guidelines for a successful submission.

1.3. If deuterated protein is required (see 2.2), neutron scattering facilities are often supported by laboratories and expertise dedicated to the production of deuterated materials. To request access to the Bio-Deuteration Lab (BDL) at ORNL, select the BDL as the second instrument in the proposal system. While the SANS proposal is reviewed for feasibility and by a scientific review committee, BDL requests are only screened for feasibility. To help with the BDL feasibility review, submit a completed information request form⁴⁸ that describes the protein expression protocol and estimated yield (available online).

1.4. After successful peer-review of the beam time proposal, confirm the awarded date of beam time in advance of the experiment. Ensure that all sample and buffer details and formulas are listed correctly in the proposal for proper review. Any changes to the proposed experimental plan, including changes in sample and buffer composition, require notification of the facility.

Note: Changes should be discussed as soon as possible with the assigned NSS.

2. Determine Neutron Contrast Match Points and Necessary Contrast for Protein Measurement

2.1. Gather information (from supplier's product information, online databases, published values, etc.) relating to atomic compositions and volumes for the detergent system components to be contrast-matched. This information is used to determine neutron scattering length densities (SLDs) and thus contrast match points (CMPs) in solution, which is critical to obtaining quality SANS data and structural information for the membrane protein of interest in the context of a PDC. A table summarizing the physical properties and contrast match points for detergents commonly used in biophysical studies of membrane proteins is included (**Table 1**).

2.2. Determine neutron SLDs using the web application MULCh: ModULes For The Analysis Of Contrast Variation Data⁴⁹ (available online⁵⁰ free-of-charge). A link to the user manual is located on the home page. Access the website and read the accompanying documentation. **Figures 1 and 2** provide an overview of Contrast module input and output for two related examples.

Note: Other websites for calculating SLDs are available, such as the one maintained by the National Institute of Standards and Technology (NIST) Center for Neutron Research⁵¹.

2.2.1. Open the Contrast module by clicking 'Contrast' located in the left navigation pane. Provide text for a project title and enter details below for two components (*e.g.*, detergent head group and tail) as 'subunit 1' and 'subunit 2'.

2.2.2. Enter the molecular formula for each component in the 'Formula' text box.

Note: The radio button 'M' must be selected under 'Substance Type' to enter a molecular formula. Additionally, use the letter 'X' in the formula to indicate readily exchangeable hydrogen atoms. Protein, RNA, or DNA sequences can be entered if the corresponding 'P', 'R', or 'D' radio buttons are selected. If multiple copies of a component exist within the subunit, the value for 'Nmolecules' can be changed accordingly. A practical example here relates to lipid-like detergents containing two identical tails, allowing the formula for one tail to be entered with Nmolecules equal to 2.

2.2.3. Enter the volume in cubic Angstroms for each component in the box below 'Volume (Å³)'. Use Tanford's formula²⁸ for alkyl chains of length n , $V_{tail} = 27.4 + n * 26.9$, to calculate approximate tail volume, or obtain molecular volumes from product information provided or published values in the literature.

2.2.4. Enter details for buffer components. Change the 'Number dissolved species in the solvent' using the dropdown menu to add or remove rows for each buffer component. In the case of micelle-forming detergents, include the free detergent monomers as separate buffer components at the detergent's critical micelle concentration (CMC).

2.2.5. Click 'Submit' to perform the neutron contrast calculations and generate a results page that provides a table of scattering length density and contrast match points as well as formulae for determining these parameters at any given percentage of D₂O in the buffer. Review the scattering parameters with particular attention to the component CMPs. If the match points are similar (within 10% D₂O) and the free micelle concentration is low, then the average CMP can be used for contrast-matching the detergent contributions. In most cases, the CMP of the detergent head group and tail will differ by more than 10-15%, producing a core-shell form factor in the SANS data which obfuscates direct collection of the scattering signal from the protein alone.

2.3. Assess the contrast between detergent head group and tail. When the detergent head group and alkyl chain tail CMPs are not well-matched, the availability and incorporation of a deuterium-

substituted detergent can permit scattering length densities of select components to be manipulated. In most cases, this will require forming a mixed micelle through the incorporation of an identical detergent with deuterium-substituted alkyl chains. The addition of deuterium raises the scattering length density of the core formed by the alkyl chain tails. The desired endpoint, in this case, is such that the head group shell CMP and alkyl chain core CMP have approximately equal values.

2.3.1. Raise the CMP of the detergent micelle core to be approximately equal to the CMP of the head group shell by determining the appropriate ratio of mixing between h-tails and d-tails that achieves complete contrast matching with the head groups. A prerequisite for this determination is knowledge of the CMP for a deuterium-substituted alkyl chain tail. A commercially-available counterpart to n-Dodecyl β -D-maltoside (DDM) is available with all alkyl chain hydrogen replaced by deuterium (d25-DDM). Repeat the contrast calculations outlined in step 2.1 for a 'd-tail' in place of the 'h-tail'.

2.3.2. Calculate the mole ratio of h-tail to d-tail required for contrast-matching with the head group CMP. The following formula can assist with this determination:

$$\text{CMP}_{\text{head}} = \text{CMP}_{\text{h-tail}} * \chi_{\text{h-tail}} + \text{CMP}_{\text{d-tail}} * \chi_{\text{d-tail}}$$

where CMP is the scattering length density and χ is the volume fraction for the detergent head, h-tail, or d-tail component. For buffered solutions of DDM, incorporation of 44% by weight (43% by mole) of the total detergent as d25-DDM with deuterium-substituted alkyl chains produces a single CMP in 48.5% D₂O for both head and tail components.

2.4. Consider the degree of deuterium substitution for the membrane protein. To measure sufficient scattering signal from the protein, the CMP for the protein should be at least 15% D₂O in solution away from the detergent CMP and measurement conditions. The signal increases with the square of this% difference. Since the CMP of an unlabeled protein typically occurs with ~42% D₂O in solution (a CMP similar to many detergent head groups), deuterium labeling of the protein is almost always a necessity⁵².

3. Express and Purify the Membrane Protein of Interest

3.1. Prepare LB (lysogeny broth) medium and grow *Escherichia coli* (*E. coli*) cells harboring an inducible expression vector for the target protein sequence.

3.1.1. Prepare minimal media. In either H₂O or D₂O, dissolve 7.0 g/L (NH₄)₂SO₄, 5.25 g/L Na₂HPO₄, 1.6 g/L KH₂PO₄, 0.50 g/L diammonium hydrogen citrate, 5.0 g/L glycerol, 1.0 mL/L of 20% w/v MgSO₄·7H₂O, and 1.0 mL/L of Holme trace metals (0.50 g/L CaCl₂·2H₂O, 0.098 g/L CoCl₂, 0.102 g/L CuSO₄, 16.7 g/L FeCl₃·6H₂O, 0.114 g/L MnSO₄·H₂O, 22.3 g/L Na₂EDTA·2H₂O, and 0.112 g/L ZnSO₄·H₂O)^{53,54}.

3.1.2. Prepare appropriate antibiotic stock solutions using H₂O or D₂O.

3.1.3. Prepare an isopropyl- β -D-1-thiogalactopyranoside stock solution using H₂O or D₂O.

3.1.4. Sterile-filter all solutions into dry, sterile containers using bottle-top vacuum and syringe filters with a 0.22 micron pore size.

3.2. Adapt *E. coli* cells to deuterium-labeled medium prior to scale-up for overexpression of a deuterated protein.

3.2.1. Inoculate 3 mL of LB medium with an isolated colony from a Lysogeny Broth (LB) agar plate or cells from a frozen glycerol stock. Grow cells at 37 °C in a shaking incubator at 250 RPM or reduce the temperature to 30 °C or below to avoid overgrowth of the culture when incubating overnight.

Note: The adaptation procedure can be varied⁵⁵⁻⁵⁷.

3.2.2. Once the LB culture has grown to an optical density at 600 nm (OD₆₀₀) of ~1, dilute it 1:20 in 3 mL of H₂O minimal medium and grow to an OD₆₀₀ of ~1. Repeat the 1:20 dilutions using minimal medium containing 50, 75 and 100% D₂O (or up to the desired D₂O percentage).

Note: As the D₂O content is increased, growth rates will decrease. The relationship between the D₂O percentage in the growth media and deuterium substitution in the protein has been reported in the literature⁵⁸⁻⁶⁰.

3.2.3. Continue growing the culture in a bioreactor to increase the yield of deuterated cell mass (Figure 3).

Note: Step-by-step procedures for bioreactor operation have been reviewed elsewhere⁶¹⁻⁶⁴.

3.3. Harvest and lyse *E. coli* cells for membrane extraction and protein purification

3.3.1. Pellet the cells by centrifugation at ~6,000 x g for ~30-45 min at 4 °C.

3.3.2. Soften the cell pellet by soaking in buffer on ice for ~30 min. Then, gently resuspend the cell pellet in buffer by gently pipetting with a serological pipet, or gentle rocking on a 2D rocker, to a final concentration of ~1 g wet cell mass/10 mL buffer.

Note: An example buffer is 50 mM HEPES (4-(2-hydroxyethyl)-1-piperazineethanesulfonic acid), pH 7.5, 200 mM NaCl supplemented with a protease inhibitor tablet.

3.3.3. Lyse resuspended cells with three passes through a high-pressure homogenizer at 10,000 psi while chilling the outflow.

Note: Depending on the scale required, other lysis methods may be used (*e.g.*, by French press or sonication).

3.3.4. Pellet cell debris by centrifugation at ~4,000 - 5,000 x g for 15 min at 4 °C. Repeat this step until the supernatant is clarified.

3.3.5. Ultracentrifuge (~150,000 x g for 30-45 min) the supernatant from the prior step, which contains the soluble and membrane fractions. The pellet after ultracentrifugation contains the membrane fraction.

3.3.6. Resuspend the membrane pellet in a large Dounce homogenizer and isolate the membrane fraction again by ultracentrifugation (step 3.2.5). Repeat this step at least once to remove loosely bound proteins.

3.3.7. Solubilize membranes by gentle rocking for ~30 min at 4 °C in a buffer containing detergent suitable for purification. Solubilization is apparent when the suspension turns from cloudy to transparent. Remove insoluble material by ultracentrifugation (~150,000 x g for 30-45 min).

Note: An example buffer is 50 mM HEPES, pH 7.5, 500 mM NaCl, 20 mM imidazole and 4% (w/v) DDM for purification by Ni²⁺ affinity chromatography.

3.4. Purify the protein following a protocol previously developed for protonated forms.

Note: See Naing *et al.* for an example purification protocol for a hexahistidine tagged *M. marisnigri* JR1 intramembrane aspartyl protease (d-MmlAP)⁶⁵. The final yield was ~ 1 mg of deuterated from 5 L deuterated cell culture growth, all of which was used in the SANS experiment (Figure 4).

3.5. Exchange the purified protein into the “Final Exchange Buffer” for contrast matching.

3.5.1. Prepare 200 mL of “Final Exchange Buffer” containing the correct mixture for contrast matching, *e.g.*, 20 mM HEPES, pH 7.5, 250 mM NaCl, and 0.05% total DDM (0.028% DDM and 0.022% d25-DDM) in 49% D₂O.

3.5.2. Equilibrate a size exclusion column with >2 column volumes (CV) of “Final Exchange Buffer” in 3.4.1 using a Fast Protein Liquid Chromatography (FPLC) system.

3.5.3. After injecting the sample, run the column and isolate fractions corresponding to the protein of interest.

3.5.4. Concentrate the protein to the desired final concentration (2 - 5 mg/mL).

Note: A volume of ~300 µL is required to fill a 1 mm cylindrical quartz cuvette used for SANS.

3.5.5. Reserve an aliquot of matched buffer for SANS background subtraction.

Note: The aliquot can be taken directly from the prepared buffer, or ideally from a clean elution

fraction at the end of the FPLC run.

4. Make Final Preparations for Beam Time and Collect SANS Data

4.1. After the proposal has been accepted and site access has been approved, complete all required training in advance of assigned beam time. This includes prearrival, web-based training as well as on-site radiological, laboratory, and instrument-specific training.

Note: Training requirements may dictate advance arrival for first time users. More information is available online⁶⁶.

4.2. Load samples and buffers for data collection.

Note: An overview of the biological small-angle neutron scattering (Bio-SANS) instrument sample environment area is shown in **Figure 5**.

4.2.1. Load samples and buffers into quartz cells. Quartz cells are available from the instrument scientist or facility. Use gel-loading tips to access the narrow opening of most sample cells.

4.2.2. Ensure that the beam shutter is closed, then approach the sample environment area and place the quartz cells in the sample changer. Record the sample changer position for each sample cell.

4.2.3. Check the area and ensure the beam path is free from obstruction, then leave the sample environment area and open the beam shutter.

Note: Carefully follow all facility rules and regulations, obey all postings, and heed advice of the instrument scientist. Samples may not be removed from the beam and manipulated after exposure to the beam without following special precautions. Consult with a Radiological Control Technician (RCT) prior to these procedures.

4.3. Execute table scan for automated data collection

4.3.1. Operate the instrument through custom control LabVIEW-based software, Spectrometer Instrument Control Environment (SpICE). Follow instructions for instrument operation provided by the Neutron Scattering Scientist. An overview of the table scan operation windows is provided in **Figure 6**.

4.3.2. After entering the information required in the appropriate areas, execute the table scan and an automated data collection process will begin. Monitor progress via the 'Table Scan Status' tab.

5. Reduce SANS Data from 2D Image to 1D Plot

5.1. Identify each sample and buffer data file from the recorded scan numbers. Each measurement will be assigned a unique scan number. This information is helpful during data reduction to identify each corresponding sample and buffer pair.

5.2. Use MantidPlot software and Python script for reduction

5.2.1. Neutron Scattering Users are provided with account details to access their data on the Remote Analysis Cluster⁶⁷. Log in to the Remote Analysis Cluster and execute “MantidPlot” from the command line. Figures 7 and 8 are provided to assist these steps.

5.2.2. Obtain a User Reduction Script from the Neutron Scattering Scientist (this will usually happen during the experiment); this script is Python-based and will contain all the necessary calibration and scaling adjustments to reduce the 2D scattering image into a 1D plot of scattered intensities as a function of scattering angle, $I(Q)$.

5.2.3. Open the provided User Reduction Script in MantidPlot and place the corresponding scan numbers or identification for the sample and buffer pairs in the appropriate list.

5.2.4. Execute the script to generate reduced data as a four-column text file (column order is Q , $I(Q)$, $I(Q)$ error, Q error) in the specified location. Right click the appropriate workspace in MantidPlot and select “Plot with errors...” for an initial examination of the scattering profiles.

6. Analyze Data for Structural Parameters of the Scattering Particle

6.1. Transfer the reduced data file from the analysis server to a local computer using secure FTP file transfer. This can be performed with the use of software such as FileZilla or CyberDuck. Additional instructions and details for connecting to the analysis server file system are provided on the analysis.sns.gov login page.

6.2. Download the ATSAS software suite^{65,68} (whole ATSAS suite⁶⁹). Individual programs⁷⁰ are also available online for analyzing the SANS data, namely determining structural parameters and *ab initio* models.

Note: Many options are available for SANS data analysis of biomacromolecules.⁴⁵

6.3. Use PRIMUS⁷¹ for data plotting, buffer scaling and subtraction, and Guinier analysis.

6.3.1. Launch the ATSAS ‘SAS Data Analysis’ application and load the reduced data files corresponding to the sample and buffer pair.

6.3.1.1. To scale the buffer properly, select a data range at high Q ($Q > 0.5 \text{ \AA}^{-1}$) where both profiles are similar and flat, and click the ‘Scale’ button located under the ‘Operations’ tab. A scale factor will be applied to the buffer such that these two flat regions should overlap. Use caution: there should be a plausible physical reason that justifies scaling the buffer intensity to match the

sample. If the discrepancy is large, consult an instrument scientist for valid approaches to background subtraction.^{44,45,72}

6.3.1.2. Increase the data range to view all points. Click 'Subtract' to perform this operation. Right click the buffer-subtracted datafile in the legend and save this file for subsequent analysis. **Figure 9** outlines the use of the 'Operations' tab.

6.3.2. Perform a Guinier analysis of the buffer-subtracted sample data using the 'Analysis' tab of the 'SAS Data Analysis' application.

6.3.2.1. Be sure the proper file is selected in the list and click 'Radius of Gyration'. An automated attempt to perform a Guinier fit will be provided by clicking on the 'Autorg' button.

6.3.2.2. Expand the range of data used to include all of the low-Q data and begin narrowing the data range by taking away high-Q points until the $Q_{\text{max}} \cdot R_g$ limit is below 1.3. Use the plot of residuals to verify that data are linear in the fit range. The Guinier fit yields an approximate R_g and I_0 for the scattering particles.

6.3.2.3. Make small adjustments to the fit region and monitor the sensitivity of these values to the range of data used in the fit. **Figure 10A** demonstrates the use of the 'Radius of Gyration' tool.

6.4. Obtain the probability distribution function ($P(r)$) in GNOM⁷³. The output file generated here will be used as an input for the *ab initio* modeling process.

6.4.1. Start the Distance Distribution Wizard within the 'Analysis' tab. Obtaining a good fit to the data is essential to obtaining a quality model. For more information on obtaining accurate fits, please see the review⁷⁴ by Putnam, *et al.*

Note: The GNOM program provides additional information about the fit beyond the Distance Distribution Wizard. **Figure 10B** demonstrates proper use of the 'Distance Distribution' tool, and **Figure 11** illustrates some of the common errors encountered.

6.4.2. Determine D_{max} , the maximum interatomic distance within the molecule.

6.4.2.1. Estimate a value for D_{max} by unchecking the box to force $R_{\text{max}}=0$ and entering a large value for D_{max} (150 Å, for example). The first x-intercept in the plot of $P(r)$ yields this estimate.

6.4.2.2. Make incremental changes to this D_{max} value and the range of data used or number of points used in the fit to optimize the GNOM fit to the data and the resulting $P(r)$ curve.

6.4.3. Continue to refine the GNOM fit and save the GNOM output files with good fit parameters for subsequent *ab initio* modeling steps.

6.5. Simulate SANS profiles from high resolution PDB models using the program CRYSON⁷⁵.

6.5.1. Open the program and select option '0'. Select the PDB file name in the popup file browser. Press enter to accept the default settings, except for specifying chain deuteration fractions and the fraction of D₂O in the solvent to achieve the proper contrast parameters.

6.5.2. Fit the model to an experimental data set by entering 'Y' and selecting the data file in the popup file browser. Accept the remaining default values, and output files will be written in the PDB file location. The '.fit' file contains information for the predicted scattering profile from the high-resolution 3D model.

7. Create *Ab Initio* Models from the SANS Data.

Note: DAMMIF⁷⁶ and DAMMIN⁷⁷ within the ATSAS software suite is used to reconstruct dummy atom models (DAMs) using a simulated annealing process from the GNOM output, which contains P(r) data, or information about the probability or frequency of interatomic distances within the scattering particle. These programs may be run in batch mode or on the ATSAS-Online web server.

7.1. Start the PRIMUS Shape Wizard from the 'Dammif' button on the 'Analysis' tab of 'SAS Data Analysis', and use a manual selection of parameters. The input for the wizard is illustrated in Figure 12.

7.1.1. Define the Guinier range from the fit (step 6.3.2) and proceed to the next step using the navigation buttons. Define fit values from the P(r) plot (step 6.4) and proceed to the next step.

7.1.2. Provide parameters for the *ab initio* modeling process. Enter a prefix for the model output filenames (e.g., SANSEnvelope), choose either 'fast' or 'slow' mode modeling, enter a value for the number of models (17 recommended for statistical significance), select from available options for particle symmetry, anisotropy, and angular scale (if known). Ensure that the boxes are checked to average models with DAMAVER and refine the final model with DAMMIN.

7.1.3. Initiate the process using the 'commit' button. Once the process is complete, view and save the working directory.

Note: The typical modeling process for a single, small protein can take up to a few hours with a typical personal computer. Files are stored in temporary directories until saved.

7.2. Overlay and superimpose the final SANS envelope with a related high-resolution model using SUPCOMB within ATSAS. Place a copy of the high-resolution PDB model to be fit to the SANS envelope in the working directory. Execute SUPCOMB from the command line using the PDB filenames as two arguments with the template structure listed first: \$ supcomb HiRes.pdb SANSEnvelope.pdb

Note: The second filename listed will be rewritten as a new file with an “r” appended to the end and having new coordinates for superimposition on the template structure.

7.3. Visualize the *ab initio* model results using PyMOL (pymol.org), a 3D molecular graphics viewing program. **Figure 13** provides an overview of the PyMOL operations.

Note: There are publication guidelines for structural modeling of small-angle scattering data from biomolecules in solution⁷⁸.

7.3.1. Launch the PyMOL application and open the .pdb files corresponding to the 3D SANS envelope and the SUPCOMB-aligned high-resolution structure to be viewed.

7.3.2. Visualize the SANS envelope by representing this model as a surface. Click the ‘S’ button next to the model and select ‘Show: As: Surface’.

7.3.3. Visualize the high-resolution protein backbone structure by representing this model as a cartoon. Select the ‘S’ button next to this model and select ‘Show: As: Cartoon’. Display the chain as a rainbow from N- to C- terminus by selecting the ‘C’ button and ‘By Chain: Chainbows’.

7.3.4. Modify the transparency of the surface representation for clarity. From the ‘Setting’ menu bar, select ‘Transparency » Surface » 40%’.

7.3.5. Make the background white and non-opaque. From the ‘Display’ menu bar, select ‘Background »’ and select ‘Opaque’ to uncheck this option and ‘White’ to mark this color for background.

Note: Additional operations and uses for PyMOL can be found at PyMolWiki.org.

REPRESENTATIVE RESULTS:

A beam time and instrument proposal should clearly convey all information needed to the review committee so that a valid assessment of the proposed experiment can be made. Communication with an NSS is highly suggested for inexperienced users. The NSS can assess initial feasibility and guide proposal submission to emphasize feasibility, safety, and the potential for high-impact science. The information provided in the proposal should include background information and context for the significance of the research; knowledge that is expected to be gained and how this impacts the current understanding in the related field of science; a description of the work, samples, methods, and procedures that will be employed; and, if applicable, previous productivity of the team at the facility, including relevant publications and results. Useful resources, such as proposal templates and tips for preparing the proposal, are available to Users via the Neutron Science User Portal (neutrons.ornl.gov/users).

Experiment planning is a dynamic process that often begins during the initial stages of proposal submission, but may not be fully conceived until just prior to the experiment. However, keep in mind that any changes that deviate significantly from the description in the proposal (including

changes to buffer conditions or sample composition) must be approved by the facility prior to the start of the experiment.

This protocol assumes that a method for expressing and purifying the membrane protein of interest into detergent micelles in solution has been successfully demonstrated. In this case, the membrane protein of interest is an intramembrane aspartyl protease (IAP), which has an established purification protocol and has been previously determined to be soluble and active in buffer containing DDM micelles.

Here, we demonstrate neutron contrast calculations using the MULCh: Contrast module for a solution of IAP protein in contrast-matched mixed DDM / d25-DDM micelles. The strategy outlined herein was to first determine the degree of mixing between the two detergents necessary to achieve a complete contrast match of the micelle. The end result was to determine the relative contrast of each component and the background (H_2O/D_2O ratio) necessary to contrast-match the scattering from detergent in order to observe only the protein scattering.

Figure 1 demonstrates a proper input for the MULCh Contrast module and the resulting output for contrast calculations of the DDM detergent head group and tail as subunits 1 and 2, respectively. The formula used for the head group is $C_{12}H_{14}X_7O_{11}$ with a volume of 348 \AA^3 , and the alkyl chain tail formula is given as $C_{12}H_{25}$ with a volume of 350 \AA^3 .

It is apparent from the Contrast module output that the DDM head group and tail have different scattering length densities, and thus contrast between the two components will be observed. For DDM, the head groups have a CMP in 49% D_2O while the alkyl chain tails have a CMP in 2% D_2O , with their average CMP occurring in 22% D_2O . Therefore, the aim of the next step will be to design a mixed micelle that incorporates deuterium-substituted alkyl chains to increase the average CMP of the detergent tails to match the CMP of the head groups. The contrast calculation was repeated for a substituted detergent, DDM with a fully-deuterated tail (d25-DDM), which similarly results in contrast between the head group and tail. However, contrast values of the h-tails and d-tails are significantly different. Recall that detergent mixtures are known to produce well-mixed micelles in solution²², thus a blend of these h- and d-tails in the micelle core should produce an average SLD equal to that of the head group shell, yielding a micelle with single CMP. Since the head group is common to both DDM and d25-DDM, the strategy is to find a mixture of these detergents that produces an average contrast value from the mixed tails that matches the contrast of the head groups.

The target average CMP for the detergent tails is that of the maltoside head groups, or 49% D_2O . To estimate the ratio of mixing the average CMP of each h-tail and d-tail component must be known. These values for some common detergents and commercially-available deuterium labelled counterparts are provided in **Table 1**. Using these CMP values for DDM and d25-DDM, the mole fraction of h-tails and d-tails that satisfies the equation provided in step 2.2 is $\chi_{d-tails} = 0.43$.

Figure 2 demonstrates a more advanced input to the MULCh Contrast module that can be used

to confirm the final mixed-micelle contrast match conditions and determine the degree of deuteration necessary on the protein. Here, subunit 1 refers to the contrast-matched mixed micelle with 2 components, DDM and d25-DDM, while subunit 2 refers to the *M. marisnigri* JR1 intramembrane aspartyl protease (MmlAP) given by its amino acid sequence. The SLD of the protein has been elevated by expression in deuterated growth media to yield a CMP for the protein in buffer containing ~92% D₂O. The degree of separation between the protein's match point in 92% D₂O and the measurement condition (48.5% D₂O) suggests that sufficient scattering signal will be obtained from the protein.

Production of d-MmlAP was carried out with Rosetta 2 *E. coli* cells harboring the pET22b-MmlAP vector. Minimal medium with unlabeled glycerol in 90% D₂O was selected as the growth medium. After adaptation to 90% D₂O minimal medium, the culture volume was scaled up to 400 mL and used to inoculate 3.6 L of fresh 90% D₂O minimal medium in a 5.5 L bioreactor vessel.

Figure 3 provides a trace of the process values during the fed-batch cultivation. At the time of inoculation, the temperature set point was 30 °C, the dissolved oxygen (DO) set point was 100%, the agitation set point was 200 rpm, and the flow rate of compressed air was 4 L/min. The pH was held above a set point of 6.9 using a 10% w/v solution of sodium hydroxide in 90% D₂O. Once the DO spike signaled depletion of the initial 5 g/L glycerol, feeding (30% w/v glycerol, 0.2% MgSO₄ in 90% D₂O) was initiated, which continued throughout the cultivation. After around 7 hours of feeding, the culture temperature was reduced to 18 °C and isopropyl-β-D-1-thiogalactopyranoside was added to a final concentration of 1 mM. Upon harvesting the culture, approximately 145 g wet weight of cell paste was collected via centrifugation (6,000 x *g* for 45 min)

Purification of d-MmlAP proceeded as for the protonated enzyme except that enzyme yield was significantly lower and final purity was somewhat lower than typical. From 5 L, ~20 g of wet membranes was isolated, all of which was solubilized in DDM for purification and loaded onto the first Ni²⁺ affinity column. To maximize purification yield, the flow-through fraction was diluted and re-rerun on Ni²⁺ affinity column. The procedure was repeated a third time before polishing the concentrated d-MmlAP sample by size exclusion chromatography (**Figure 4**).

Figure 5 depicts a quartz sample cell and its related sample changer setup. Sample environments are managed by the Bio-SANS operations team and NSS. A variety of different environments can be arranged to perform measurements with temperature control, humidity control, mechanical tumbling, high temperature, and sustained pressure, among others.

Figure 6 demonstrates Bio-SANS operations and execution of the automated table scans. The table scan is configured to be intuitive and user-friendly. On the first tab (Load Samples), information is provided about the sample changer and setup, such as identification of samples at each position in the sample changer, cell thicknesses, and sample type (open beam, sample, background, etc.). Additional metadata tags can be applied here also. On the next tab (Plan Experiment), the instrument configuration and any associated parameters (such as temperature control) are defined. This step is arranged by the NSS at the start of the experiment. The user

must simply input the measurement times for each sample (in seconds). The final tab (Execute Scans) provides a summary of the table scan data and allows the automated scan to be executed.

After the 2D scattering images are recorded, this data must be reduced to a 1D plot of the intensity versus Q – a function of the scattering angle. During data reduction, image corrections such as pixel sensitivity masks and dark background subtractions are also applied. MantidPlot software was designed to interpret the raw Bio-SANS instrument data. The NSS will generally assist in reducing and retrieving the final data at the end of the experiment.

Figure 7 provides an overview of the remote analysis cluster access to MantidPlot and the Script Window used for data reduction. Raw data are accessible at the remote analysis cluster (analysis.sns.gov) via UCAMS/XCAMS user authentication. After logging into the remote desktop, the MantidPlot software can be launched from a terminal window by simply executing 'MantidPlot' under any path. Open the Script Window in MantidPlot and edit the User Reduction Script as directed by the NSS. Executing this script will generate the reduced data files, which can then be transferred to a local machine for analysis using secure FTP.

Figure 8 demonstrates plotting and viewing the data after executing the User Reduction Script. Reduced data will appear in the Workspaces window. By default, final merged data will have the suffix `_f` appended. Right-click will allow Plot Spectrum with Errors to be selected and data to be plotted. Display preferences are accessed by selecting Preferences from the 'View' menu bar. Formatting of axes and plotting range is easily accessible by double-clicking the axes. Scattering profiles of buffers, which contain no scattering particles of significant size should appear as a relatively flat line (constant intensity). For samples, intensity should be observed at lower scattering angles (Q) with exponential decay to a flat incoherent background.

Figure 9 provides an overview of proper buffer subtraction using the SAS Data Analysis (or primusqt) software package following data reduction. Quite often the incoherent background (intensity at high- Q) is slightly mismatched between the sample and buffer. For proper subtraction, data in this region should overlap. The scale correction applies an intensity scale factor to the data which results in overlapping data, and the subtraction can be performed. If the scale factor results in buffer data points with larger intensity than corresponding points in the sample, then these points will be negative and not rendered in a log plot. If negative values in the buffer-subtracted file are abundant, make a minor reduction in the buffer scale factor and perform the subtraction again.

Figure 10 provides example usages of the Primus Guinier and Distance Distribution Wizards. A Guinier analysis provides a preliminary estimate of the particles radius of gyration from the low-angle scattering data. As data approach zero, a linear region should be present in the data. Fitting of a line in this region allows the R_g to be determined from the slope and an I_0 to be extrapolated from the intensity intercept at $Q=0$. An upward trend in the data as Q approaches zero indicates aggregation in the sample, while downward trends are usually indicative of interparticle repulsions. These trends are most apparent when the distribution of residuals is non-stochastic. The upper limit of the Guinier fit for globular particles is constrained by $Q \cdot R_g < 1.3$ ('s' is used in

place of Q in the ATSAS software).

The R_g determined for d-MmIAP from this Guinier fit was $15.4 \pm 1.1 \text{ \AA}$ with an estimated I_0 given as 0.580 ± 0.001 .

The distance distribution wizard allows systematic changes to be made to parameters of the $P(r)$ fit. The $P(r)$ curve is an indirect Fourier transform of the curve fit to the experimental data. Therefore, it is essential to verify that the fit in the left panel accurately reflects the experimental data. For the fit shown in this example, a D_{max} of 46 \AA was obtained.

Figure 11 illustrates common errors in D_{max} selection. A D_{max} that is artificially large often causes $P(r)$ values to become negative as the $P(r)$ function oscillates about the x-axis. A D_{max} that is artificially small leads to a truncated $P(r)$ curve with an abrupt transition to $R_{\text{max}}=0$.

The first steps in the Primus Shape Wizard are identical to the Guinier and Distance Distribution Wizards. Once this information has been provided to obtain good fits to the experimental data, the *ab initio* model setup is configured.

Figure 12 illustrates a proper input for the Primus Shape Wizard. Here, experimental SANS data for the IAP was provided with a scale in Angstroms, and the expected file prefix of "SANSEnvelope" was given. A set of 17 initial dummy atom models were requested to be generated using "fast" model mode with no symmetry (P1) applied and no anisotropy selected. The set of 17 models will be aligned, averaged, and filtered with DAMAVER, and the average model refined using DAMMIN. Inspection of the *prefix-damsel.log* text document provides a summary of the selection criterion and any models discarded from the set. The final refined model was written as SANSEnvelope-1.pdb.

The program SUPCOMB is used to perform a superimposition of the SANS envelope model with the high-resolution model, with only the two PDB structure files as input. By default, "r" is appended to the reoriented and superimposed file name.

Once the SANS envelope and high-resolution structure have been superimposed, these models can be visualized using any molecular graphics viewing program. The results from PyMOL are suitable for publication quality images and can be used to emphasize biophysical results relating to the structural investigation. Here, we demonstrate a few basic PyMOL operations used to provide 3D representations and views of the resulting superimposed structures.

Figure 13 provides an overview of the PyMOL visualization process. Once the PDB structure files have been opened in PyMOL, the models should be visible in the PyMOL Viewer window. Change the representations of each model using the 'S' button next to each file name. Use a surface representation for the SANS envelope and a cartoon representation of the protein backbone from the high-resolution model. Select a suitable color scheme from options available under the 'C' button. For protein chains, a "chainbow" coloring provides a color gradient from N- to C-terminus to aid interpretation. Transparency is applied to the surface representation to allow

better visualization of the protein structure within the envelope. For publication images, a white background is recommended. Once these visualization queues have been applied, the 3D structures can be examined. Manipulations of the perspective and molecule rotation/translation can be performed by clicking and dragging the structure.

FIGURE AND TABLE LEGENDS:

Figure 1. Usage of the MULCh Contrast module to determine contrast parameters for components of dodecyl maltoside (DDM). Input values are shown in the screen on the left with the subsequent output to the right. The Contrast module input page is accessed by clicking 'Contrast' (green circle) from the navigation menu on the left side of each screen. Input areas for the project title, buffer components, and subunits 1 and 2 are labelled as such. Output pages contain important particle information and contrast properties for the described system. Relevant tables and calculated match points have been boxed in orange for clarity.

Figure 2. Usage of the MULCh Contrast module to determine contrast parameters for components of the membrane protein-detergent complex. In this instance, input has been given to describe the overall PDC system in buffered solution. Subunit 1 describes the contrast-matched mixed micelle composed of DDM with 43% by mole as d25-DDM. Subunit 2 describes the membrane protein, with the amino acid sequence for MmIAP input as the formula. The deuteration level (green circle) describes the protein's degree of deuterium substitution, and has a direct impact on the SLD and calculated match-point that will be estimated for the protein. Results (orange box) indicate that match-point for the mixed detergent will occur in 48.5% D₂O, while the protein's match-point occurs at ~90% D₂O.

Figure 3. Sample preparation – Bioreactor trace. The process values displayed are temperature set point (orange line), dissolved oxygen (DO) set point (blue line), agitation set point (red line), and compressed air flow rate (pink line). Pump 1 (green line) was used for pH control. The DO spike at 18:40 signaled depletion of the initial glycerol and was used to initiate feeding of glycerol solution via pump 2 (black line). X-axis denotes hours.

Figure 4. Sample preparation – FPLC and SDS-PAGE characterization of the sample. Final size exclusion chromatogram for *d*-MmIAP equilibrated with 20 mM HEPES, pH 7.5, 250 mM NaCl, 48.5% D₂O and 0.05% total DDM, of which 44% (w/v) is tail-deuterated d25-DDM. Inset: SDS-PAGE analysis with Coomassie staining. Pooled fractions are labeled A, B, and C. Region "B" was used in the SANS experiment. Annotated molecular weight marker is in kDa. Image reproduced with permission from Naing *et al.*⁶⁵.

Figure 5. Data collection – Quartz banjo sample cell and autosampler setup. (A) An empty quartz banjo cell is shown resting against the autosampler block. Cells are filled with sample and inserted into one of the 15 available positions. **(B)** The sample block is mounted behind an aperture selector (not shown) between the Beam Tube Extender and Silicon window at the entrance to the detector tank. Hoses connecting to a temperature-controlled water bath and channels throughout the sample block provide temperature regulation at the sample positions. The arrow indicates the direction of the neutron beam.

Figure 6. Data Collection – Overview of SPICE operations and table scan. The table scan operations are accessible from the 'Table Scan' button on the far left menu of the SPICE instrument control software. Green arrows denote the active tab at the top of the screen and orange boxes highlight areas in the table for active user inputs. **(A)** The first tab of the table scan is used to provide information about the sample changer and sample cell positions. Provide labels, sample thicknesses, and sample types for each position used in the sample changer. Checking the 'Do Scan' box will add the corresponding row to the table scan queue. **(B)** On the second tab, details about the instrument configuration and measurement time for each sample (in seconds) are recorded. Instrument configurations are preconfigured by the Neutron Scattering Scientist and provided to users based on details provided in the beam time and instrument proposal. Additional parameters can be added to the instrument control, such as the ability to define temperature setpoints and hold times, throughout the measurement queue. **(C)** The final tab provides an overview of the measurements to be made for each row in the table. If no changes are needed, the automated scan is initiated by clicking the 'Execute Scans' button.

Figure 7. Data Reduction – Overview of reduction script and MantidPlot operations. MantidPlot software is accessible on the analysis cluster by typing "mantidplot" in a terminal command prompt at any active directory (the yellow circle and arrow are added for emphasis). Once the software is open, access the script window (toggled by button marked in green) and open the script provided by the Neutron Scattering Scientist. Follow the instructions provided in the script, which should only require the scan numbers for each sample and buffer to be entered in a list for automated reduction, as well as scan numbers for the empty cell for subtraction and empty beam for transmission and beam center determination.

Figure 8. Data Analysis – Plotting of data using MantidPlot. Data are referenced as 'Workspaces' in MantidPlot. The workspace area will be populated with filenames as produced by the user reduction script. Workspace data for 1D data sets can be plotted by right-clicking the workspace and selecting "Plot Spectrum with Errors...". Additional data can be added to the current plot by simply dragging and dropping workspaces. Formatting of the plot window (such as for log-log plots) can be performed by selecting 'Preferences' from the 'View' menu bar, or double-clicking on the axis labels.

Figure 9. Data Analysis – ATSAS software: basic operations and buffer subtraction. The primusqt application (SAS Data Analysis) provides visualization for proper background (buffer) subtraction. The buffer file should be scaled for subtraction such that data overlap at high-Q (where scattering is flat as a result of remaining signal from incoherent background). When this high-Q range of data is selected, the Scale operation will apply a scale factor to the lower data file in the table that produces overlap in the defined region. After scaling, the buffer file can be subtracted to yield the net scattering profile of the particle.

Figure 10. Data Analysis – Guinier and P(r) (distance distribution) determination. (A) The Primus Guinier Wizard is used to perform a Guinier analysis, providing an initial estimate of I_0 and R_g . The particle type and range of data to fit are used to define the fit. A plot of the fit and corresponding

residuals are shown to the left, while Guinier terms (I_0 and R_g), $Q \cdot R_g$ limits, and quality of linear fit are provided as output in the area marked by the orange box. **(B)** The Primus Distance Distribution Wizard is used to perform the distance distribution analysis, providing the $P(r)$ curve which defines the probability of interatomic distances within the scattering particle and includes the D_{max} or maximum interatomic distance. Parameters indicated by the orange box can be systematically investigated to determine a proper distance distribution function.

Figure 11. Improper results from the distance distribution analysis. A properly selected D_{max} should produce a $P(r)$ curve that peaks with a gradual decay to zero. D_{max} values that are too large will likely produce negative $P(r)$ values or oscillations near the x-axis at high values of r . D_{max} values that are artificially small often result in $P(r)$ curves where the upper bound appears truncated.

Figure 12. Modeling – *Ab initio* model setup using the Primus Shape Wizard. *Ab initio* modeling parameters are provided in a single input window. A prefix is supplied for output file names with other options for processing available. Annealing procedure can be fast (bigger beads with faster cooling) or slow (smaller beads with slower cooling). Number of repetitions should be of sufficient size to examine reproducibility of model features. Particle symmetry and anisotropy can be provided, if known. Angular scale should correspond to the units of the measured data. DAMAVER averaging will align and average all dummy atom models, and then apply a selection criterion which excludes any outlier models. A core of fixed atoms from the averaged model will be further refined using DAMMIN if this option is selected. This refined model should represent the 3D low-resolution envelope of the experimental SANS profile.

Figure 13. Visualization – Experimental SANS envelope and overlay with high-resolution model using PyMOL. After opening the PDB structure files in PyMOL, models appear in the PyMOL Viewer. Active models are listed in the table to the right, along with action buttons which can be used to manipulate the model and its representation. Basic operations are provided for visualizing these models which allow regions of agreement (or mismatch) between the SANS envelope and high-resolution structure to be identified.

Table 1. Physical properties of detergents commonly used in membrane protein investigations.

DISCUSSION:

Structural biology researchers take advantage of complementary structural techniques like solution scattering to obtain biochemical and structural details (such as overall size and shape) from biomolecules in solution. SANS is a particularly attractive technique for determining low resolution structures of membrane proteins, a core focus of modern structural biology and biochemistry. SANS requires quantities of purified proteins comparable to those of crystallographic trials (1 mg/sample). The recently expanding commercial availability of high-purity deuterated detergents relevant to membrane protein studies makes accessible a means to manipulate this hydrogen/deuterium content for SANS experiments of membrane protein-detergent complexes, allowing the protein signal to be recorded directly. When successful, an *ab initio* model molecular envelope can be calculated from data collected over just several hours.

Thus, membrane protein biochemists, biophysicists, and structural biologists can readily take advantage of SANS to obtain coveted initial 3D models of membrane proteins in solution, structures in complex with binding partners or substrates, and models obtained by SANS can be used for phasing diffraction data. Routine usage of SANS to characterize membrane proteins would be transformative for the membrane protein biochemistry field and have ripple effects from basic structure function to drug discovery and development. The added advantage of neutron contrast matching with deuterium substitution makes SANS a valuable technique for studying protein-protein, protein-DNA, or other biomolecular complexes, which can be readily manipulated in their hydrogen/deuterium content.

For additional details about small-angle scattering instrument design and theory, the following reviews are recommended: The Bio-SANS instrument at the High Flux Isotope Reactor of Oak Ridge National Laboratory⁷⁹, Small-angle scattering for structural biology – expanding the frontier while avoiding the pitfalls⁷², and Small-angle scattering studies of biological macromolecules in solution⁸⁰. The Neutron Scattering Scientist can also discuss current instrument configurations and the optimal parameters for a given system. In, data at lower Q (which is a function of the scattering angle and neutron wavelength) is generally desired for larger systems. The most common instrument configuration at Bio-SANS provides a Q_{\min} of 0.003 \AA^{-1} and is suitable for larger protein complexes up to hundreds of kDa. A solution containing $\sim 3 \text{ mg mL}^{-1}$ of membrane protein of approximate size of 30 kDa (monomer) in contrast-matched micelles with 48.5% D_2O in solution requires a typical measurement time around 8 hours each for sample, buffer, and empty cell (24 hours = 1day total). Instrument measurement times at a given contrast condition can be approximately scaled according to the product of the scattering particle's molecular mass and concentration. However, scattering particles must be measured under non-interacting conditions, including any non-specific protein aggregation, which places a practical upper limit on the concentration of the sample. Hour-long measurements place limits on the stability of certain proteins. Fortunately, SANS measurements can be done routinely at refrigerated temperatures to improve protein life time, and the employed beam of low-energy neutrons does not cause any radiation damage during the measurement.

An overview of this process and determination of many key factors toward the successful recording of the neutron scattering from a sample measured at the contrast match point of the detergent are presented in this manuscript. This includes the critical step toward obtaining a complete match of the aggregate detergent by designing a detergent mixture with a uniform neutron contrast between the detergent head group and alkyl chain components. Measurements at this single detergent match point provide a scattering profile attributed to only the membrane protein of interest and allowed an *ab initio* envelope representing the membrane protein to be reconstructed from the data. The data analysis and *ab initio* modeling protocols also demonstrate the potential information obtained from such investigations, which could aim to address overall structure, conformational changes, oligomeric states, among others. One limitation is that to date only very few detergents are commercially available with deuterium substitutions¹⁹.

While perdeuteration may not be necessary, the aim in this case should be to achieve a protein with >65% deuterium labeling in the protein. Alternatively, if detergent with selectively-

deuterated head groups and tails is available, and the CMP of the detergent micelle occurs near 100% D₂O, then sufficient contrast from the protein can be achieved without the need for deuterium labeling. Determine the appropriate deuteration level of the protein to achieve sufficient scattering when measured at the contrast-match point of the detergent. There are numerous challenges associated with membrane protein expression and purification⁸¹, which remain beyond the scope of this article. Unfortunately, high levels of deuteration are currently not (yet) possible for eukaryotic systems. While we realize this is a limitation for some eukaryotic proteins, most membrane proteins have bacterial orthologs for which this method is suitable.

ACKNOWLEDGMENTS:

The Office of Biological and Environmental Research supported research at ORNL's Center for Structural Molecular Biology (CSMB) and Bio-SANS using facilities supported by the Scientific User Facilities Division, Office of Basic Energy Sciences, US Department of Energy. Structural work on membrane proteins in the Lieberman lab has been supported by NIH (DK091357, GM095638) and NSF (0845445).

DISCLOSURES:

The authors Volker S. Urban, Sai Venkatesh Pingali, Kevin L. Weiss, and Ryan C. Oliver are contracted through UT-Battelle with US DOE to support the Neutron Science User Program and Bio-SANS instrument at Oak Ridge National Laboratory used in this Article.

This manuscript has been co-authored by UT-Battelle, LLC, under contract DE-AC05-00OR22725 with the US Department of Energy (DOE). The US government retains and the publisher, by accepting the article for publication, acknowledges that the US government retains a nonexclusive, paid-up, irrevocable, worldwide license to publish or reproduce the published form of this manuscript, or allow others to do so, for US government purposes. DOE will provide public access to these results of federally sponsored research in accordance with the DOE Public Access Plan⁸².

REFERENCES:

- 1 Wallin, E. & Heijne, G. V. Genome-wide analysis of integral membrane proteins from eubacterial, archaean, and eukaryotic organisms. *Protein Science*. **7** (4), 1029-1038, doi:10.1002/pro.5560070420, (1998).
- 2 Tautermann, C. S. GPCR structures in drug design, emerging opportunities with new structures. *Bioorganic & Medicinal Chemistry Letters*. **24** (17), 4073-4079, doi:10.1016/j.bmcl.2014.07.009, (2014).
- 3 Cournia, Z. *et al.* Membrane protein structure, function, and dynamics: A perspective from experiments and theory. *The Journal of Membrane Biology*. **248** (4), 611-640, doi:10.1007/s00232-015-9802-0, (2015).
- 4 Doerr, A. Membrane protein structures. *Nature Methods*. **6** 35, doi:10.1038/nmeth.f.240, (2008).
- 5 Bill, R. M. *et al.* Overcoming barriers to membrane protein structure determination. *Nature Biotechnology*. **29** 335, doi:10.1038/nbt.1833, (2011).
- 6 Carpenter, E. P., Beis, K., Cameron, A. D. & Iwata, S. Overcoming the challenges of

969 membrane protein crystallography. *Current Opinion in Structural Biology*. **18** (5), 581-586,
970 doi:10.1016/j.sbi.2008.07.001, (2008).

971 7 Sanders, C. R. & Sönnichsen, F. Solution NMR of membrane proteins: Practice and
972 challenges. *Magnetic Resonance in Chemistry*. **44** (S1), S24-S40, doi:10.1002/mrc.1816,
973 (2006).

974 8 Garavito, R. M. & Ferguson-Miller, S. Detergents as tools in membrane biochemistry.
975 *Journal of Biological Chemistry*. **276** (35), 32403-32406, doi:10.1074/jbc.R100031200,
976 (2001).

977 9 Privé, G. G. Detergents for the stabilization and crystallization of membrane proteins.
978 *Methods*. **41** (4), 388-397, doi:10.1016/j.ymeth.2007.01.007, (2007).

979 10 Wessel, D. & Flügge, U. I. A method for the quantitative recovery of protein in dilute
980 solution in the presence of detergents and lipids. *Analytical Biochemistry*. **138** (1), 141-
981 143, doi:10.1016/0003-2697(84)90782-6, (1984).

982 11 Bayburt, T. H., Grinkova, Y. V. & Sligar, S. G. Self-assembly of discoidal phospholipid bilayer
983 nanoparticles with membrane scaffold proteins. *Nano Letters*. **2** (8), 853-856,
984 doi:10.1021/nl025623k, (2002).

985 12 Bayburt, T. H. & Sligar, S. G. Membrane protein assembly into Nanodiscs. *FEBS Letters*.
986 **584** (9), 1721-1727, doi:10.1016/j.febslet.2009.10.024, (2010).

987 13 Skar-Gislinge, N. *et al.* Elliptical structure of phospholipid bilayer nanodiscs encapsulated
988 by scaffold proteins: Casting the roles of the lipids and the protein. *Journal of the*
989 *American Chemical Society*. **132** (39), 13713-13722, doi:10.1021/ja1030613, (2010).

990 14 Sanders, C. R. & Schwonek, J. P. Characterization of magnetically orientable bilayers in
991 mixtures of dihexanoylphosphatidylcholine and dimyristoylphosphatidylcholine by solid-
992 state NMR. *Biochemistry*. **31** (37), 8898-8905, doi:10.1021/bi00152a029, (1992).

993 15 Vestergaard, M., Kraft, J. F., Vosegaard, T., Thøgersen, L. & Schiøtt, B. Bicelles and other
994 membrane mimics: comparison of structure, properties, and dynamics from MD
995 simulations. *The Journal of Physical Chemistry B*. **119** (52), 15831-15843,
996 doi:10.1021/acs.jpcb.5b08463, (2015).

997 16 Popot, J.-L. *et al.* Amphipols From A to Z. *Annual Review of Biophysics*. **40** (1), 379-408,
998 doi:10.1146/annurev-biophys-042910-155219, (2011).

999 17 Tribet, C., Audebert, R. & Popot, J.-L. Amphipols: Polymers that keep membrane proteins
1000 soluble in aqueous solutions. *Proceedings of the National Academy of Sciences*. **93** (26),
1001 15047, doi:n/a, (1996).

1002 18 Fernández, C. & Wüthrich, K. NMR solution structure determination of membrane
1003 proteins reconstituted in detergent micelles. *FEBS Letters*. **555** (1), 144-150,
1004 doi:10.1016/S0014-5793(03)01155-4, (2003).

1005 19 Hiruma-Shimizu, K., Shimizu, H., Thompson, G. S., Kalverda, A. P. & Patching, S. G.
1006 Deuterated detergents for structural and functional studies of membrane proteins:
1007 Properties, chemical synthesis and applications. *Molecular Membrane Biology*. **32** (5-8),
1008 139-155, doi:10.3109/09687688.2015.1125536, (2015).

1009 20 Krueger-Koplin, R. D. *et al.* An evaluation of detergents for NMR structural studies of
1010 membrane proteins. *Journal of Biomolecular NMR*. **28** (1), 43-57,
1011 doi:10.1023/B:JNMR.0000012875.80898.8f, (2004).

1012 21 Linke, D. in *Methods in Enzymology* Vol. 463 eds Richard R. Burgess & Murray P.

Deutscher) 603-617 (Academic Press, 2009).

22 Oliver, R. C. *et al.* Tuning micelle dimensions and properties with binary surfactant mixtures. *Langmuir*. **30** (44), 13353-13361, doi:10.1021/La503458n, (2014).

23 Orwick-Rydmark, M., Arnold, T. & Linke, D. The use of detergents to purify membrane proteins. *Current Protocols in Protein Science*. **84** (1), 4.8.1-4.8.35, doi:10.1002/0471140864.ps0408s84, (2016).

24 Tanford, C. & Reynolds, J. A. Characterization of membrane proteins in detergent solutions. *Biochimica et Biophysica Acta (BBA) - Reviews on Biomembranes*. **457** (2), 133-170, doi:10.1016/0304-4157(76)90009-5, (1976).

25 Tulumello, D. V. & Deber, C. M. Efficiency of detergents at maintaining membrane protein structures in their biologically relevant forms. *Biochimica et Biophysica Acta (BBA) - Biomembranes*. **1818** (5), 1351-1358, doi:10.1016/j.bbamem.2012.01.013, (2012).

26 Arachea, B. T. *et al.* Detergent selection for enhanced extraction of membrane proteins. *Protein Expression and Purification*. **86** (1), 12-20, doi:10.1016/j.pep.2012.08.016, (2012).

27 Seddon, A. M., Curnow, P. & Booth, P. J. Membrane proteins, lipids and detergents: Not just a soap opera. *Biochimica et Biophysica Acta (BBA) - Biomembranes*. **1666** (1), 105-117, doi:10.1016/j.bbamem.2004.04.011, (2004).

28 Tanford, C. *The Hydrophobic Effect: Formation of Micelles and Biological Membranes*. 2nd edn, (John Wiley, 1980).

29 Littrell, K., Urban, V., Tiede, D. & Thiyagarajan, P. Solution structure of detergent micelles at conditions relevant to membrane protein crystallization. *Journal of Applied Crystallography*. **33** (3 Part 1), 577-581, doi:10.1107/S002188989901314X, (2000).

30 Oliver, R. C. *et al.* Dependence of micelle size and shape on detergent alkyl chain length and head group. *PLOS ONE*. **8** (5), e62488, doi:10.1371/journal.pone.0062488, (2013).

31 le Maire, M., Champeil, P. & Møller, J. V. Interaction of membrane proteins and lipids with solubilizing detergents. *Biochimica et Biophysica Acta (BBA) - Biomembranes*. **1508** (1), 86-111, doi:10.1016/S0304-4157(00)00010-1, (2000).

32 Hong, X., Weng, Y.-X. & Li, M. Determination of the topological shape of integral membrane protein light-harvesting complex LH2 from photosynthetic bacteria in the detergent solution by small-angle X-ray scattering. *Biophysical Journal*. **86** (2), 1082-1088, doi:10.1016/S0006-3495(04)74183-1, (2004).

33 Vinothkumar, K. R. Membrane protein structures without crystals, by single particle electron cryomicroscopy. *Current Opinion in Structural Biology*. **33** 103-114, doi:10.1016/j.sbi.2015.07.009, (2015).

34 Pérez, J. & Koutsioubas, A. Memprot: A program to model the detergent corona around a membrane protein based on S-SAXS data. *Acta Crystallographica Section D*. **71** (1), 86-93, doi:10.1107/S1399004714016678, (2015).

35 Oliver, R. C., Pingali, S. V. & Urban, V. S. Designing mixed detergent micelles for uniform neutron contrast. *The Journal of Physical Chemistry Letters*. **8** (20), 5041-5046, doi:10.1021/acs.jpclett.7b02149, (2017).

36 Hiruma-Shimizu, K., Kalverda, A. P., Henderson, P. J. F., Homans, S. W. & Patching, S. G. Synthesis of uniformly deuterated n-dodecyl- β -D-maltoside (d39-DDM) for solubilization of membrane proteins in TROSY NMR experiments. *Journal of Labelled Compounds & Radiopharmaceuticals*. **57** (14), 737-743, doi:10.1002/jlcr.3249, (2014).

1057 37 Midtgaard, S. R. *et al.* Invisible detergents for structure determination of membrane
1058 proteins by small-angle neutron scattering. *The FEBS Journal*. **285** (2), 357-371,
1059 doi:10.1111/febs.14345, (2018).

1060 38 Gabel, F. in *Biological Small Angle Scattering: Techniques, Strategies and Tips* eds Barnali
1061 Chaudhuri, Inés G. Muñoz, Shuo Qian, & Volker S. Urban) 201-214 (Springer Singapore,
1062 2017).

1063 39 Schantz, A. B. *et al.* PEE–PEO Block copolymer exchange rate between mixed micelles is
1064 detergent and temperature activated. *Macromolecules*. **50** (6), 2484-2494,
1065 doi:10.1021/acs.macromol.6b01973, (2017).

1066 40 Liyana-Arachchi, T. P. *et al.* Bubble bursting as an aerosol generation mechanism during
1067 an oil spill in the deep-sea environment: Molecular dynamics simulations of oil alkanes
1068 and dispersants in atmospheric air/salt water interfaces. *Environmental Science:
1069 Processes & Impacts*. **16** (1), 53-64, doi:10.1039/C3EM00391D, (2014).

1070 41 Dos Santos Morais, R. *et al.* Contrast-matched isotropic bicelles: A versatile tool to
1071 specifically probe the solution structure of peripheral membrane proteins using SANS.
1072 *Langmuir*. **33** (26), 6572-6580, doi:10.1021/acs.langmuir.7b01369, (2017).

1073 42 Maric, S. *et al.* Stealth carriers for low-resolution structure determination of membrane
1074 proteins in solution. *Acta Crystallographica Section D*. **70** (2), 317-328,
1075 doi:10.1107/S1399004713027466, (2014).

1076 43 Pedersen, J. S., Svaneborg, C., Almdal, K., Hamley, I. W. & Young, R. N. A small-angle
1077 neutron and x-ray contrast variation scattering study of the structure of block copolymer
1078 micelles: Corona shape and excluded volume interactions. *Macromolecules*. **36** (2), 416-
1079 433, doi:10.1021/ma0204913, (2003).

1080 44 Urban, V. S. in *Characterization of Materials* (ed Elton N. Kaufmann) (John Wiley and Sons,
1081 2012).

1082 45 Chaudhuri, B., Muñoz, I. G., Qian, S. & Urban, V. S. in *Advances in Experimental Medicine
1083 and Biology* Vol. 1009 (eds Irun R. Cohen *et al.*) 1-268 (Springer Singapore, Singapore,
1084 2017).

1085 46 Neutron Facilities WorldWide, <http://neutronsources.org>.

1086 47 Submitting a Research Proposal, <https://neutrons.ornl.gov/users/proposals>.

1087 48 Accompanying Bio-Deuteration Laboratory Proposal,
1088 https://www.ornl.gov/sites/default/files/BDL_info_request.docx (2014).

1089 49 Whitten, A. E., Cai, S. & Trewella, J. MULCh: Modules for the analysis of small-angle
1090 neutron contrast variation data from biomolecular assemblies. *Journal of Applied
1091 Crystallography*. **41** (1), 222-226, doi:10.1107/S0021889807055136, (2008).

1092 50 MULCh: ModULes for the Analysis of Contrast Variation Data, [http://smb-
1093 research.smb.usyd.edu.au/NCVWeb/](http://smb-research.smb.usyd.edu.au/NCVWeb/).

1094 51 Scattering Length Density Calculator by National Institute of Standards and Technology
1095 (NIST) Center for Neutron Research, [https://www.ncnr.nist.gov/resources/activation/
1096 \(2018\)](https://www.ncnr.nist.gov/resources/activation/).

1097 52 Ibel, K. & Stuhmann, H. B. Comparison of neutron and X-ray scattering of dilute
1098 myoglobin solutions. *Journal of Molecular Biology*. **93** (2), 255-265, doi:10.1016/0022-
1099 2836(75)90131-X, (1975).

1100 53 Holme, T., Arvidson, S., Lindholm, B. & Pavlu, B. Enzymes: Laboratory-scale production.

1101 *Process Biochemistry*. **5** (9), 62-66, doi:n/a, (1970).

1102 54 Törnkvist, M., Larsson, G. & Enfors, S.-O. Protein release and foaming in *Escherichia coli*
 1103 cultures grown in minimal medium. *Bioprocess Engineering*. **15** (5), 231-237,
 1104 doi:10.1007/bf02391583, (1996).

1105 55 Artero, J.-B., Hartlein, M., McSweeney, S. & Timmins, P. A comparison of refined X-ray
 1106 structures of hydrogenated and perdeuterated rat [gamma]E-crystallin in H₂O and D₂O.
 1107 *Acta Crystallographica Section D*. **61** (11), 1541-1549, doi:10.1107/S0907444905028532,
 1108 (2005).

1109 56 Paliy, O., Bloor, D., Brockwell, D., Gilbert, P. & Barber, J. Improved methods of cultivation
 1110 and production of deuteriated proteins from *E. coli* strains grown on fully deuteriated
 1111 minimal medium. *Journal of applied microbiology*. **94** (4), 580-586, doi:10.1046/j.1365-
 1112 2672.2003.01866.x, (2003).

1113 57 Sivashanmugam, A. *et al.* Practical protocols for production of very high yields of
 1114 recombinant proteins using *Escherichia coli*. *Protein Science*. **18** (5), 936-948,
 1115 doi:10.1002/pro.102, (2009).

1116 58 Hoopes, J. T., Elbersen, M. A., Preston, R. J., Reddy, P. T. & Kelman, Z. in *Methods in*
 1117 *Enzymology* Vol. 565 (ed Zvi Kelman) 27-44 (Academic Press, 2015).

1118 59 Leiting, B., Marsilio, F. & O'Connell, J. F. Predictable deuteration of recombinant proteins
 1119 expressed in *Escherichia coli*. *Analytical Biochemistry*. **265** (2), 351-355,
 1120 doi:10.1006/abio.1998.2904, (1998).

1121 60 Perkins, S. J. Estimation of deuteration levels in whole cells and cellular proteins by ¹H
 1122 n.m.r. spectroscopy and neutron scattering. *Biochemical Journal*. **199** (1), 163-170,
 1123 doi:n/a, (1981).

1124 61 Obom, K. M., Magno, A. & Cummings, P. J. Operation of a benchtop bioreactor. *Journal of*
 1125 *Visualized Experiments*. (79), e50582, doi:10.3791/50582, (2013).

1126 62 Duff, A. P., Wilde, K. L., Rekas, A., Lake, V. & Holden, P. J. in *Methods in Enzymology* Vol.
 1127 565 (ed Zvi Kelman) 3-25 (Academic Press, 2015).

1128 63 Haertlein, M. *et al.* in *Methods in Enzymology* Vol. 566 (ed Zvi Kelman) 113-157 (Academic
 1129 Press, 2016).

1130 64 Meilleur, F., Weiss, K. L. & Myles, D. A. A. in *Micro and Nano Technologies in Bioanalysis*
 1131 Vol. 544 *Methods in Molecular Biology* 281-292 (2009).

1132 65 Naing, S.-H., Oliver, R. C., Weiss, K. L., Urban, V. S. & Lieberman, R. L. Solution structure
 1133 of an intramembrane aspartyl protease via small angle neutron scattering. *Biophysical*
 1134 *Journal*. **114** (3), 602-608, doi:10.1016/j.bpj.2017.12.017, (2018).

1135 66 Training Requirements for First Time and Repeat Users, <https://neutrons.ornl.gov/users>.
 1136 67 Remote Analysis Cluster, <https://analysis.sns.gov>.

1137 68 Franke, D. *et al.* ATSAS 2.8: A comprehensive data analysis suite for small-angle scattering
 1138 from macromolecular solutions. *Journal of Applied Crystallography*. **50** (4), 1212-1225,
 1139 doi:10.1107/S1600576717007786, (2017).

1140 69 ATSAS Software Suite, <https://www.embl-hamburg.de/biosaxs/download.html>.

1141 70 ATSAS Software Individual Programs, [https://www.embl-](https://www.embl-hamburg.de/biosaxs/software.html)
 1142 [hamburg.de/biosaxs/software.html](https://www.embl-hamburg.de/biosaxs/software.html).

1143 71 Konarev, P. V., Volkov, V. V., Sokolova, A. V., Koch, M. H. J. & Svergun, D. I. PRIMUS: A
 1144 Windows PC-based system for small-angle scattering data analysis. *Journal of Applied*

1145 *Crystallography*. **36** (5), 1277-1282, doi:10.1107/S0021889803012779, (2003).

1146 72 Jacques, D. A. & Trewella, J. Small-angle scattering for structural biology—Expanding the
 1147 frontier while avoiding the pitfalls. *Protein Science*. **19** (4), 642-657, doi:10.1002/pro.351,
 1148 (2010).

1149 73 Svergun, D. Determination of the regularization parameter in indirect-transform methods
 1150 using perceptual criteria. *Journal of Applied Crystallography*. **25** (4), 495-503,
 1151 doi:10.1107/S0021889892001663, (1992).

1152 74 Putnam, C. D., Hammel, M., Hura, G. L. & Tainer, J. A. X-ray solution scattering (SAXS)
 1153 combined with crystallography and computation: defining accurate macromolecular
 1154 structures, conformations and assemblies in solution. *Quarterly Reviews of Biophysics*. **40**
 1155 (3), 191-285, doi:10.1017/S0033583507004635, (2007).

1156 75 Svergun, D. I. *et al.* Protein hydration in solution: Experimental observation by x-ray and
 1157 neutron scattering. *Proceedings of the National Academy of Sciences of the United States*
 1158 *of America*. **95** (5), 2267-2272, doi:n/a, (1998).

1159 76 Franke, D. & Svergun, D. I. DAMMIF, a program for rapid ab-initio shape determination in
 1160 small-angle scattering. *Journal of Applied Crystallography*. **42** (2), 342-346,
 1161 doi:10.1107/S0021889809000338, (2009).

1162 77 Svergun, D. I. Restoring Low Resolution Structure of Biological Macromolecules from
 1163 Solution Scattering Using Simulated Annealing. *Biophysical Journal*. **76** (6), 2879-2886,
 1164 doi:10.1016/S0006-3495(99)77443-6, (1999).

1165 78 Jacques, D. A., Guss, J. M., Svergun, D. I. & Trewella, J. Publication guidelines for
 1166 structural modelling of small-angle scattering data from biomolecules in solution. *Acta*
 1167 *Crystallographica Section D*. **68** (6), 620-626, doi:10.1107/S0907444912012073, (2012).

1168 79 Heller, W. T. *et al.* The Bio-SANS instrument at the High Flux Isotope Reactor of Oak Ridge
 1169 National Laboratory. *Journal of Applied Crystallography*. **47** (4), 1238-1246,
 1170 doi:10.1107/S1600576714011285, (2014).

1171 80 Svergun, D. I. & Koch, M. H. J. Small-angle scattering studies of biological macromolecules
 1172 in solution. *Reports on Progress in Physics*. **66** (10), 1735, doi:10.1088/0034-
 1173 4885/66/10/R05, (2003).

1174 81 Johnson, J. L., Kalyoncu, S. & Lieberman, R. L. in *Heterologous Expression of Membrane*
 1175 *Proteins: Methods and Protocols* (ed Isabelle Mus-Veteau) 281-301 (Springer New York,
 1176 2016).

1177 82 Department of Energy Public Access Plan, [http://energy.gov/downloads/doe-public-](http://energy.gov/downloads/doe-public-access-plan)
 1178 [access-plan](http://energy.gov/downloads/doe-public-access-plan).

1179

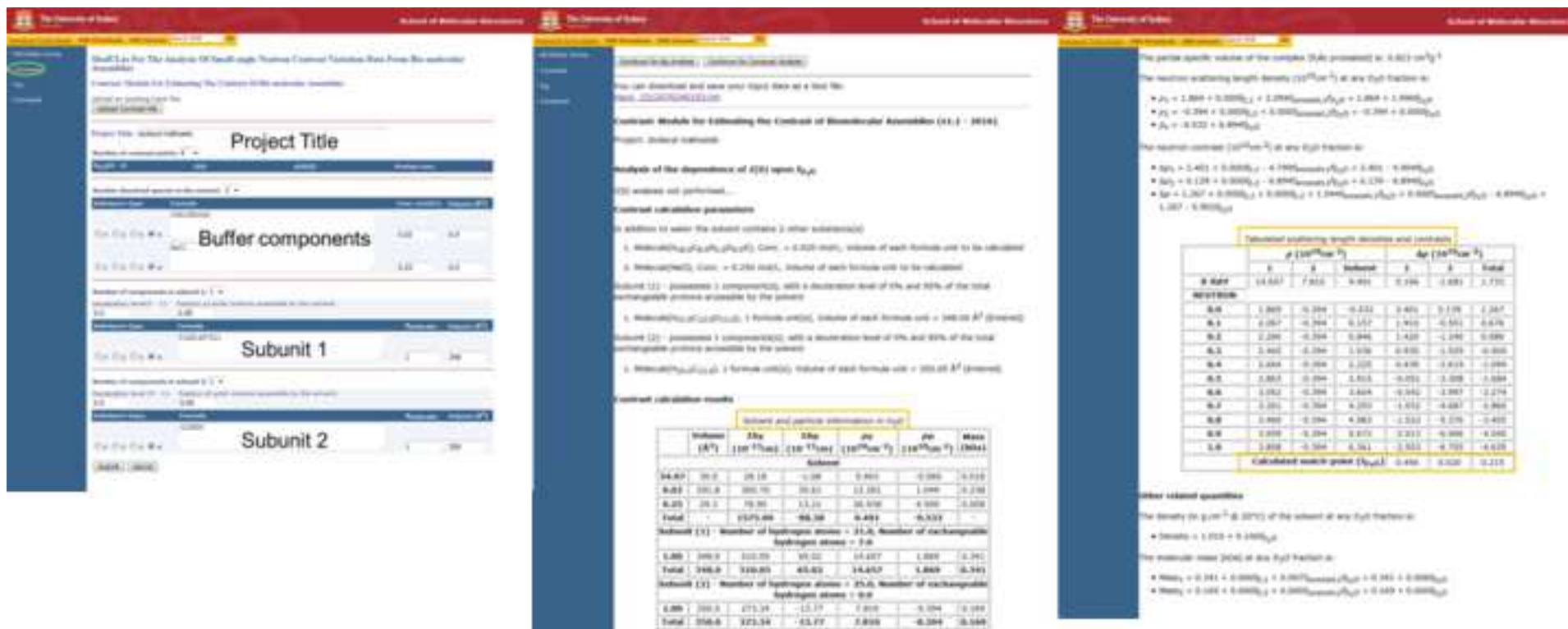
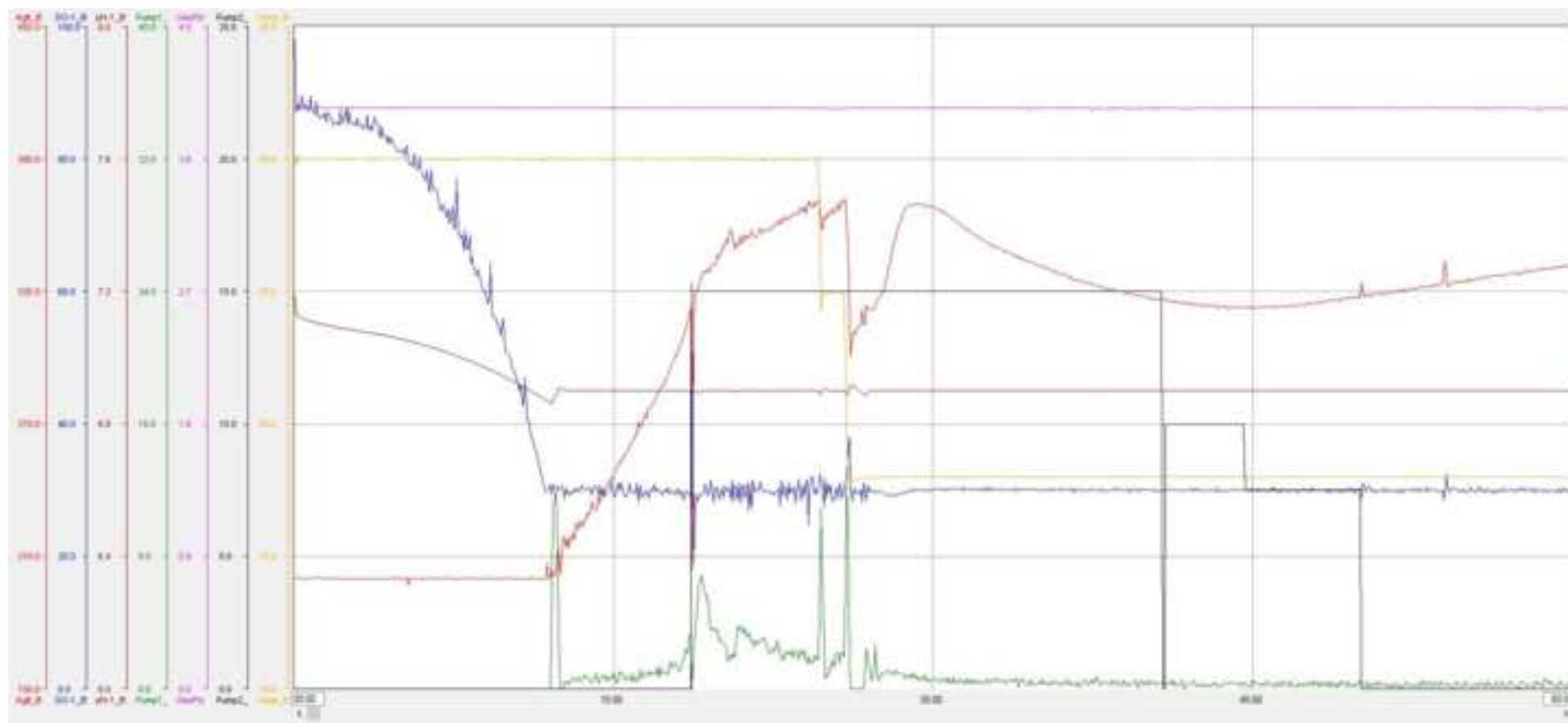
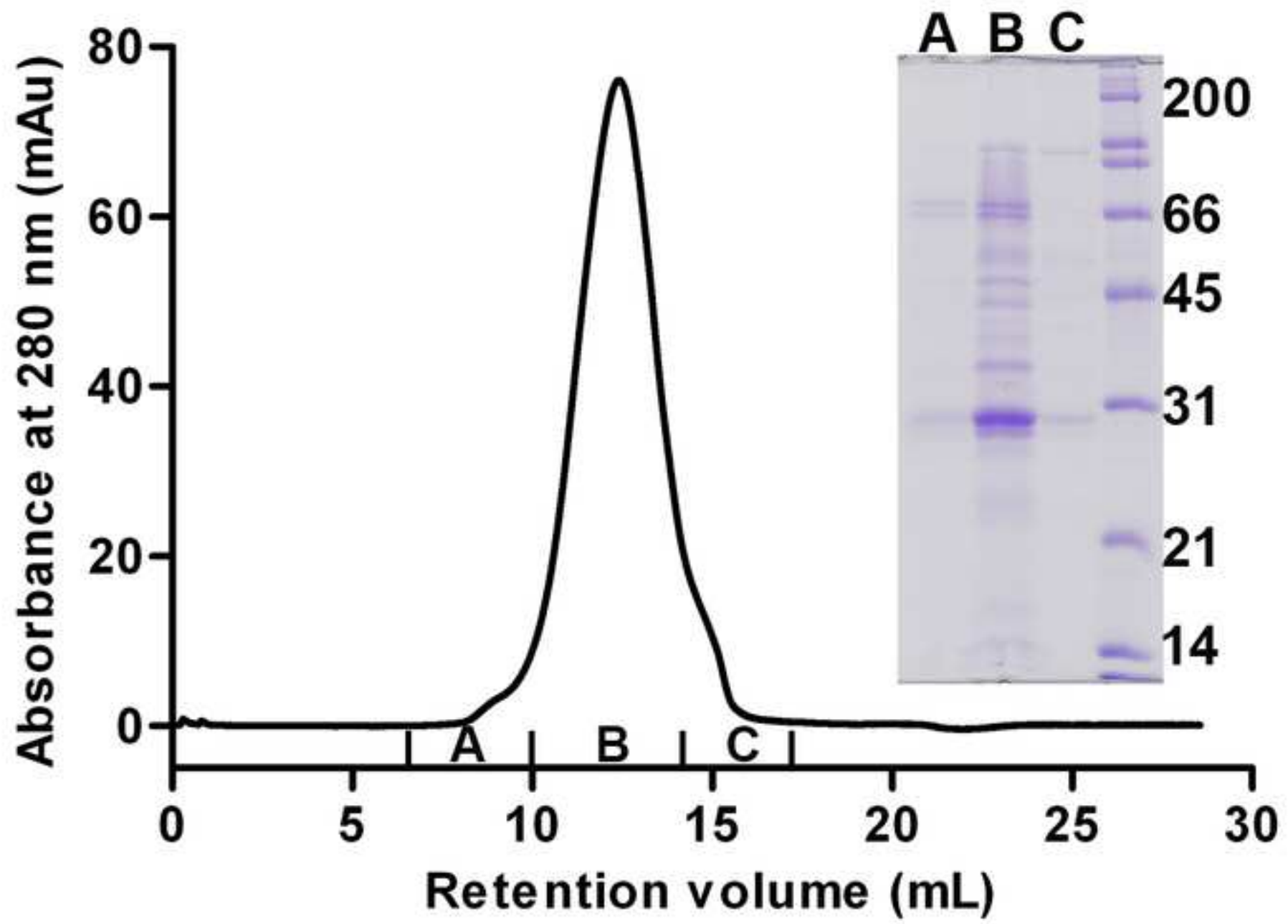




Figure 3

[Click here to download Figure Figure3.tif](#)





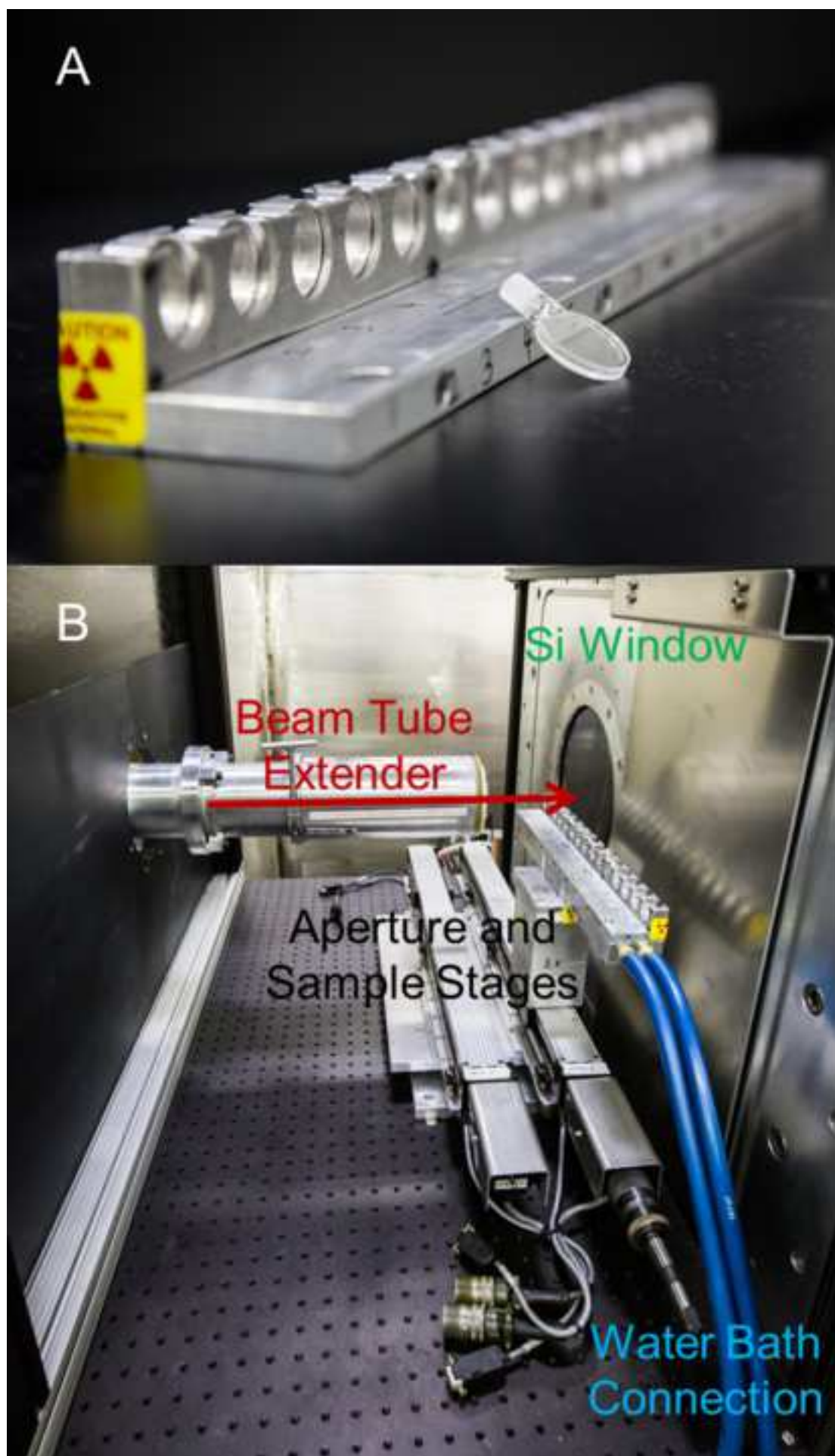


Figure 6 displays three screenshots (A, B, and C) of a software interface for managing sample scans.

Screenshot A: The "Load Samples" tab is active. The "Sample Changer List" is highlighted, showing a table of samples. The "Sample Changer" dropdown is set to "Sample". The "Sample Manager Columns" and "Background Manager Columns" buttons are visible.

Position #	Sample ID	Sample Name	Sample Thickness (mm)	Sample Type	Ex Time
1	001	Open Beam	0	Open Beam	25
2	002	Empty Cell	0	Empty Cell	25
3	003	Sample	0	Sample	25
4	004	Buffer	0	Background	25
5	005		0	Sample	25
6	006		0	Sample	25
7	007		0	Sample	25
8	008		0	Sample	25
9	009		0	Sample	25
10	010		0	Sample	25
11	011		0	Sample	25
12	012		0	Sample	25
13	013		0	Sample	25
14	014		0	Sample	25

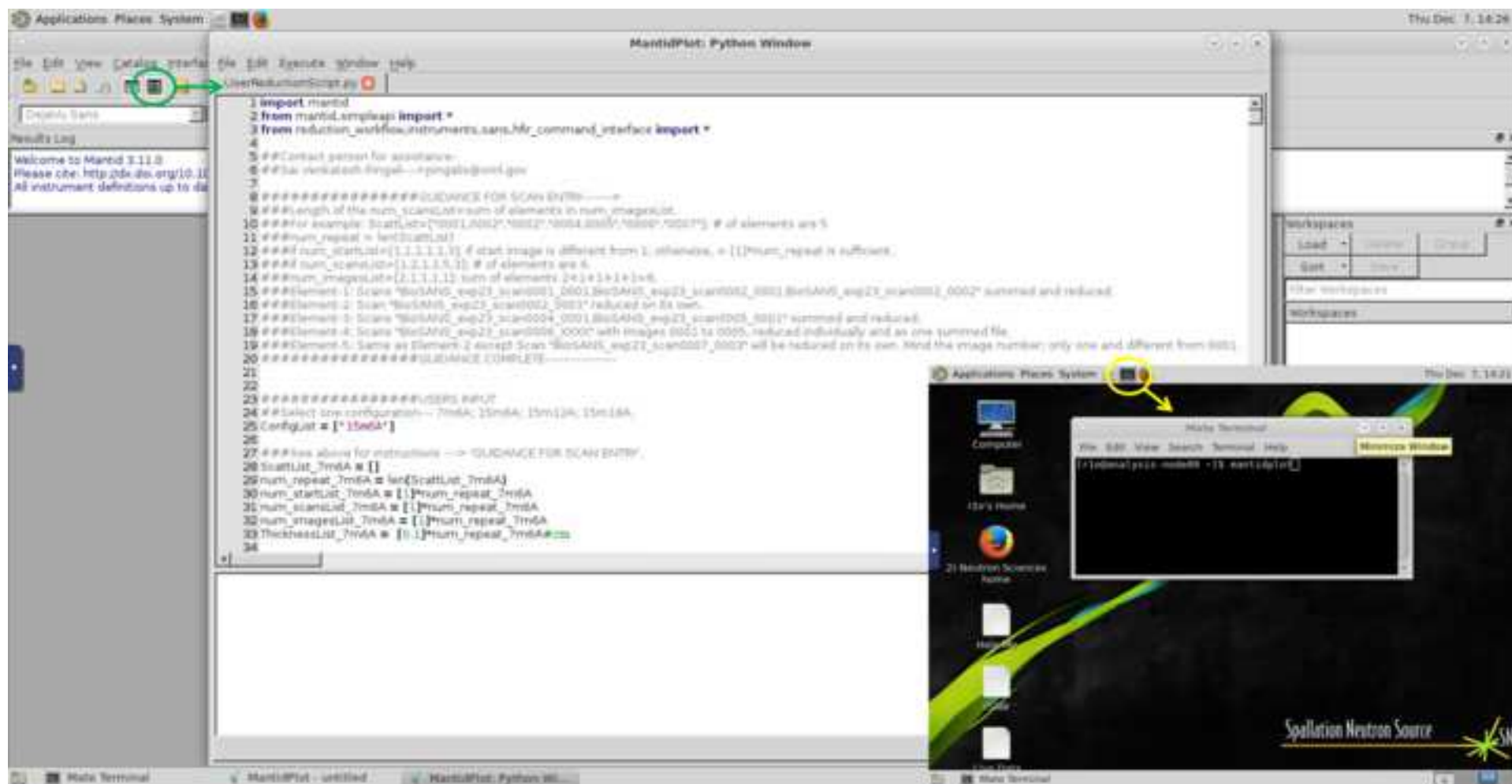
Screenshot B: The "Plan Experiment" tab is active. The "Sample Changer" dropdown is set to "Sample". The "Background Setup Order" is set to "0.001-0.0". The "Scan Order" dropdown is set to "Scan Order". The "Estimated Scan Time" is 06:21:00. The "Sample Manager Columns" and "Background Manager Columns" buttons are visible.

Position #	Sample Name	Sample Type	Scan Time
1	Open Beam	Open Beam	25
2	Empty Cell	Empty Cell	25
3	Sample	Sample	25
4	Buffer	Background	25

Screenshot C: The "Execute Scans" tab is active. The "Execute Scans" button is highlighted. The "Estimated Total Scan Time" is 00:21:00. The "Sample Manager Columns" and "Background Manager Columns" buttons are visible.

Scan #	Position #	Sample ID	Sample Name	Sample Type	Scan Type	Scan Name	Scan Time	Frame Count	Estimated Total Scan Time
112	1	001	Open Beam	Open Beam	Scan	0.001-0.0	25	1	00:21:00
113	2	002	Empty Cell	Empty Cell	Scan	0.001-0.0	25	1	00:21:00
114	3	003	Sample	Sample	Scan	0.001-0.0	25	1	00:21:00
115	4	004	Buffer	Background	Scan	0.001-0.0	25	1	00:21:00

Figure 7

[Click here to download Figure Figure7.tif](#)

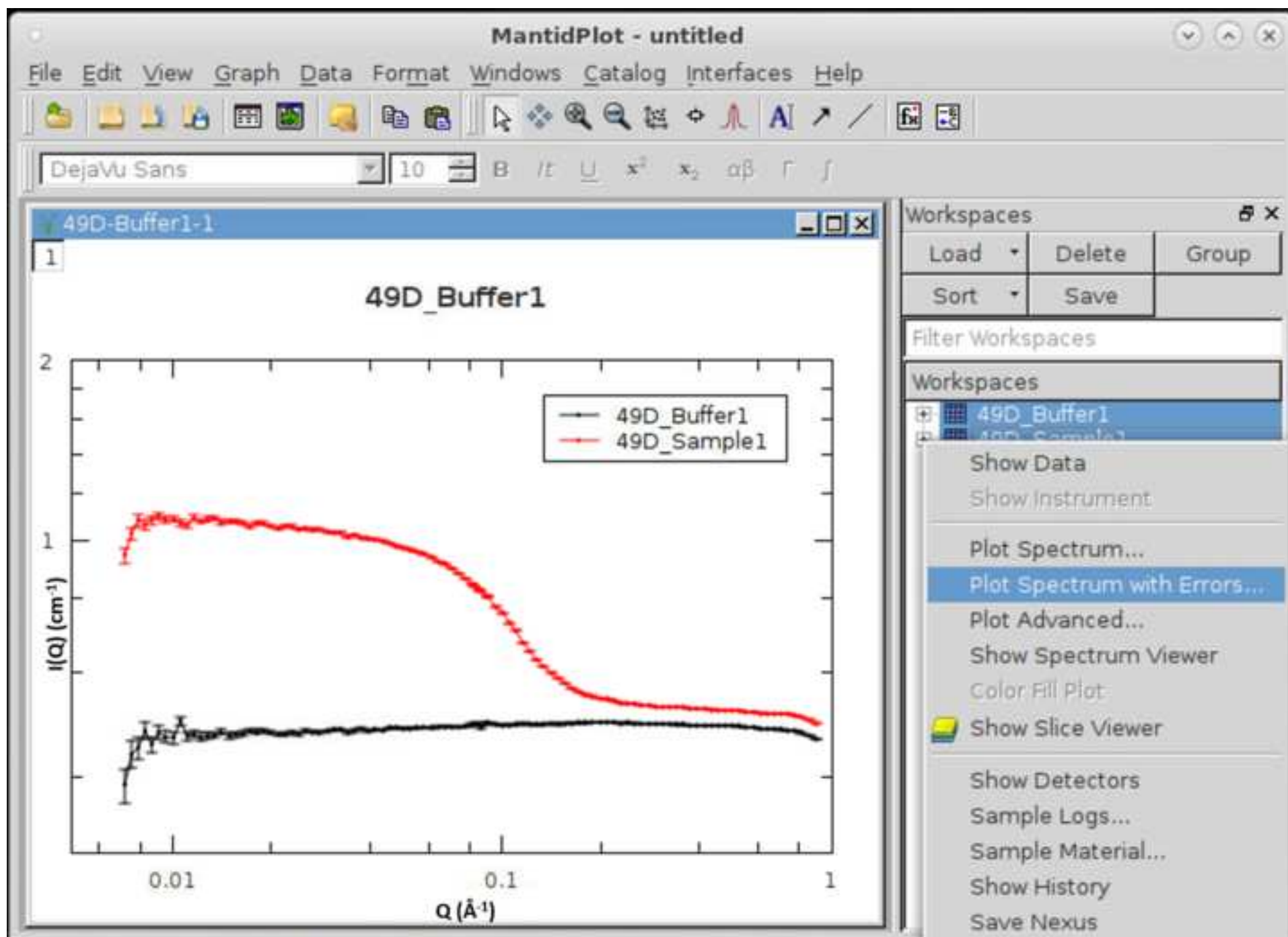
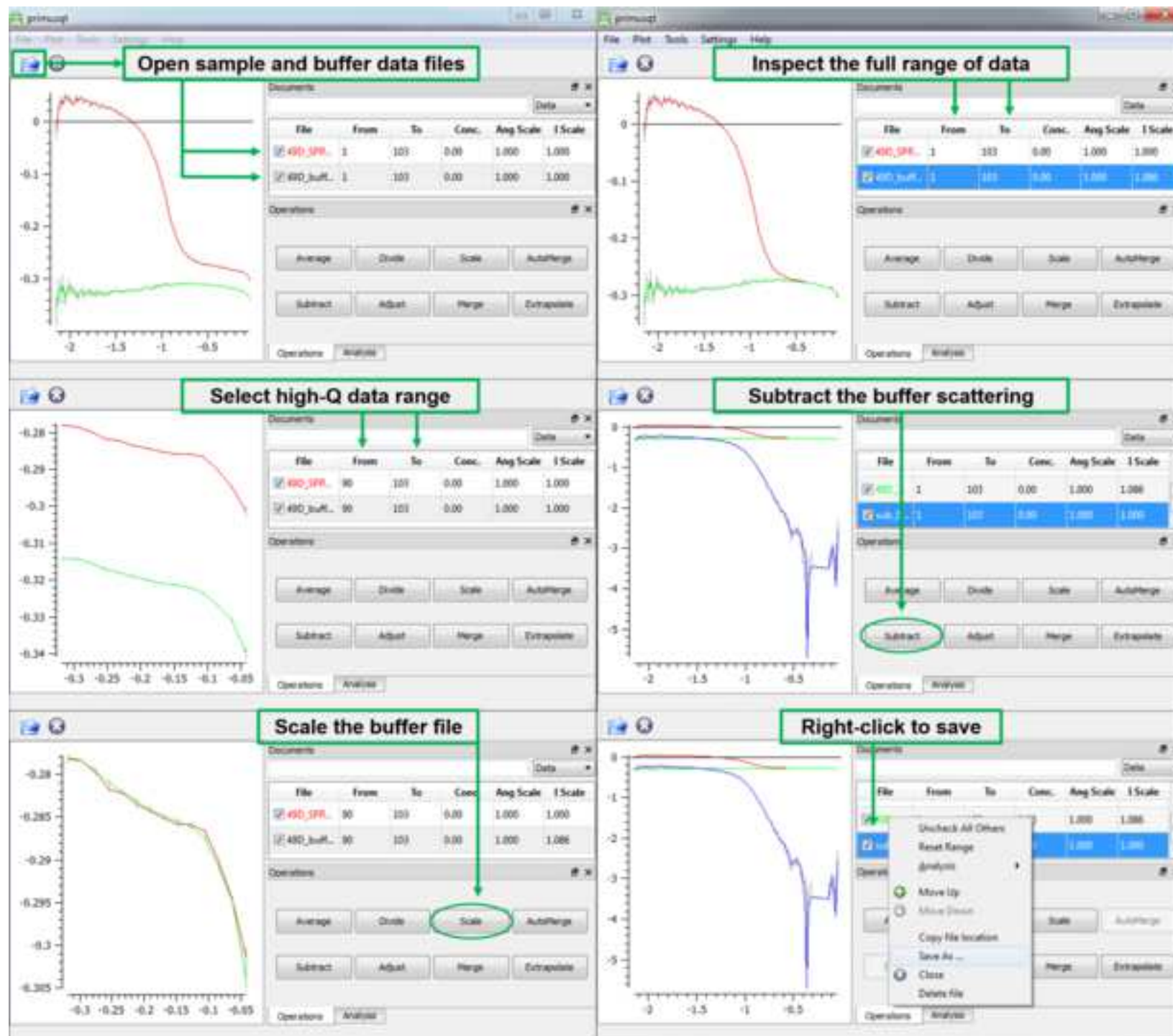
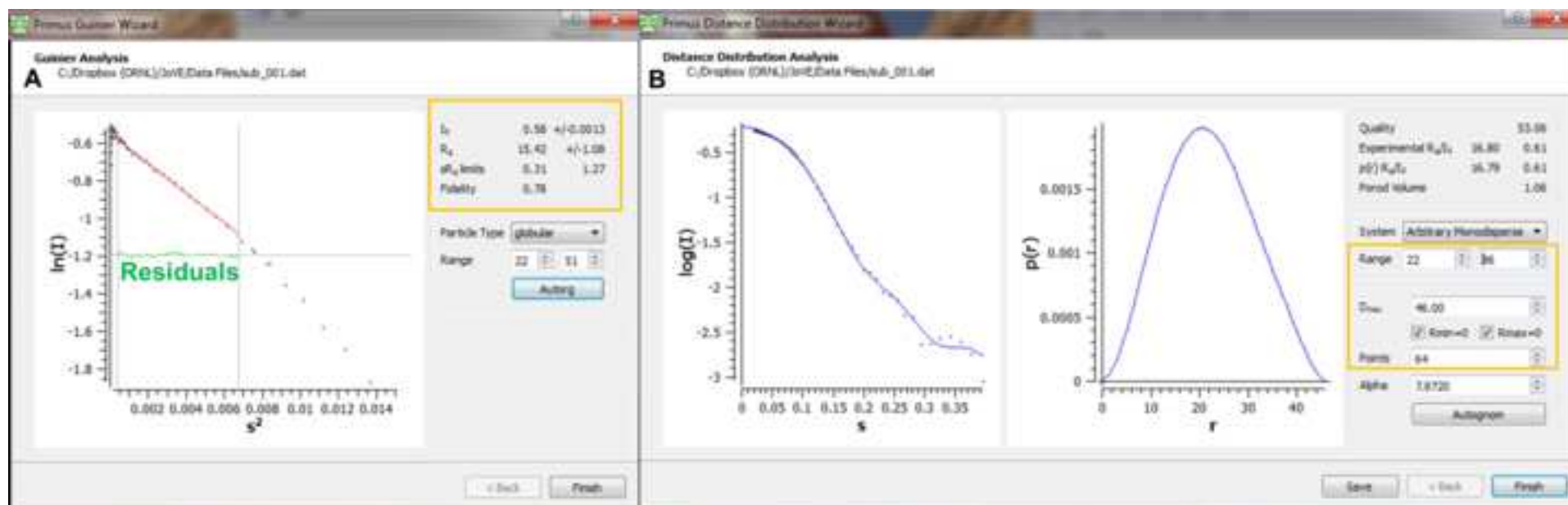
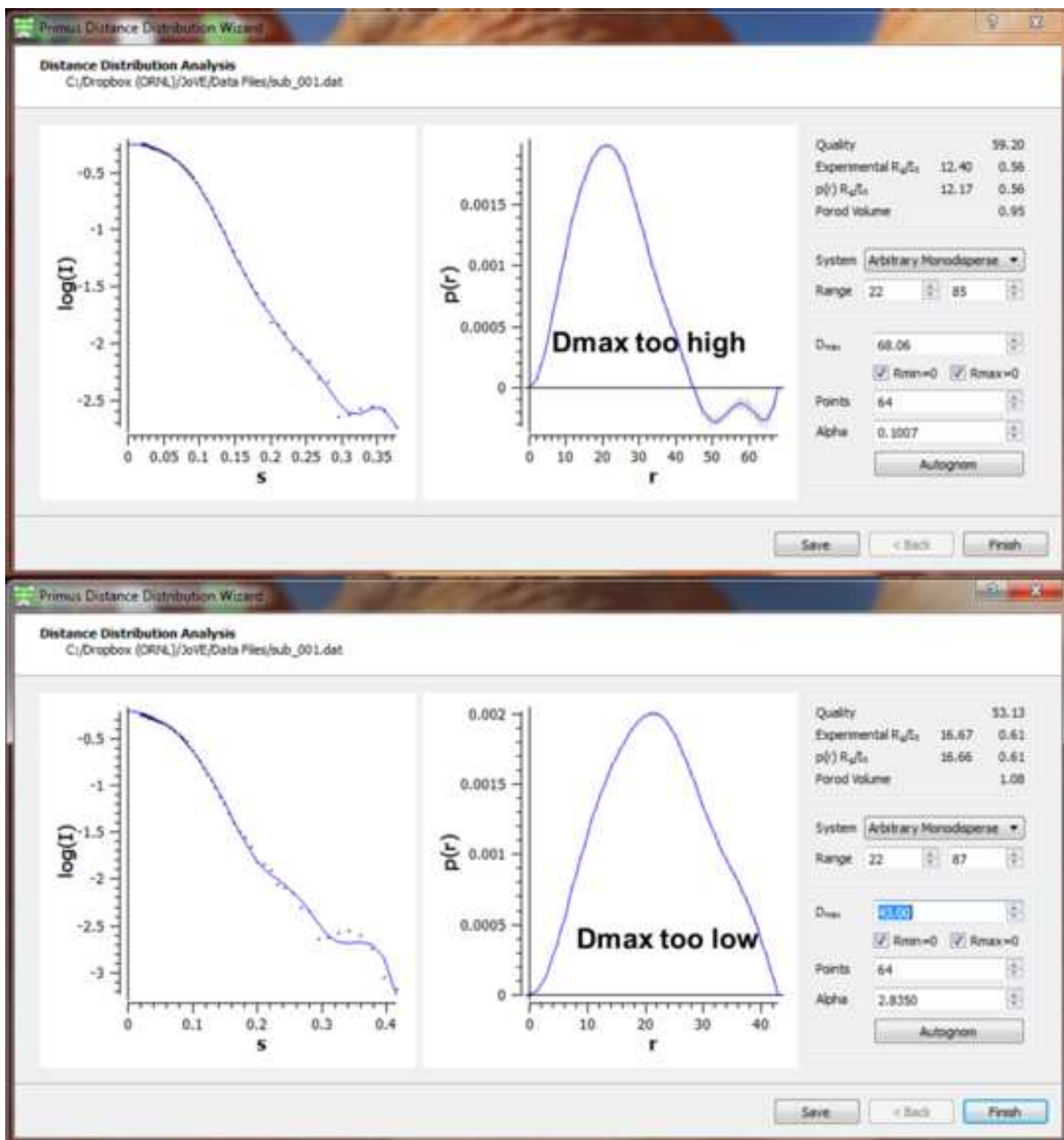
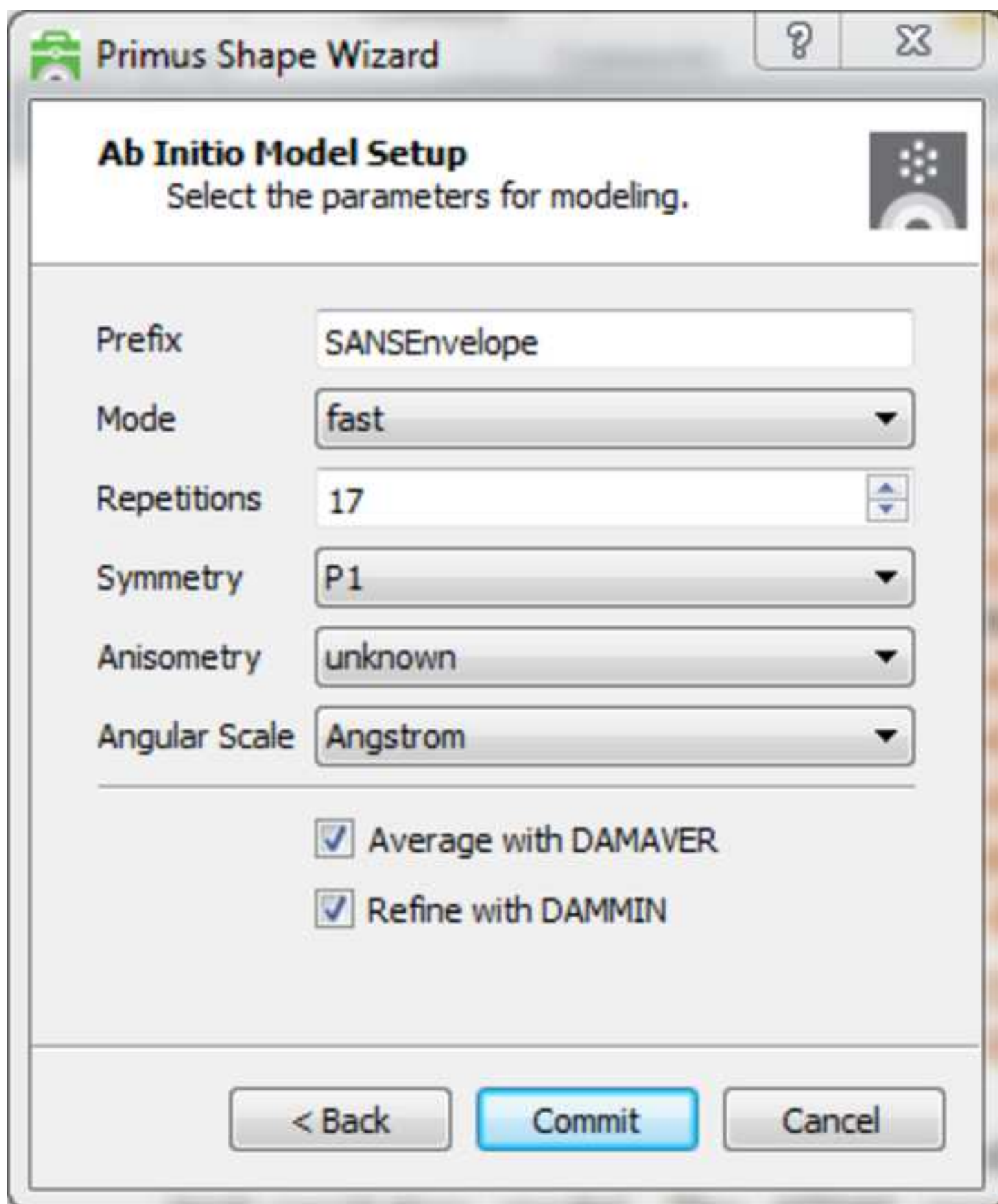


Figure 9

[Click here to download Figure Figure9_new.tif](#)







The image shows a software dialog box titled "Primus Shape Wizard". It has a standard window header with a question mark icon and a close button. The main title is "Ab Initio Model Setup" with a subtitle "Select the parameters for modeling." and a small icon of a crystal structure. The dialog contains several input fields and checkboxes. The "Prefix" field is a text box containing "SANSEnvelope". The "Mode" field is a dropdown menu showing "fast". The "Repetitions" field is a text box with "17" and a spin button. The "Symmetry" field is a dropdown menu showing "P1". The "Anisometry" field is a dropdown menu showing "unknown". The "Angular Scale" field is a dropdown menu showing "Angstrom". Below these fields are two checked checkboxes: "Average with DAMAVER" and "Refine with DAMMIN". At the bottom are three buttons: "< Back", "Commit" (highlighted in blue), and "Cancel".

Primus Shape Wizard

Ab Initio Model Setup
Select the parameters for modeling.

Prefix: SANSEnvelope

Mode: fast

Repetitions: 17

Symmetry: P1

Anisometry: unknown

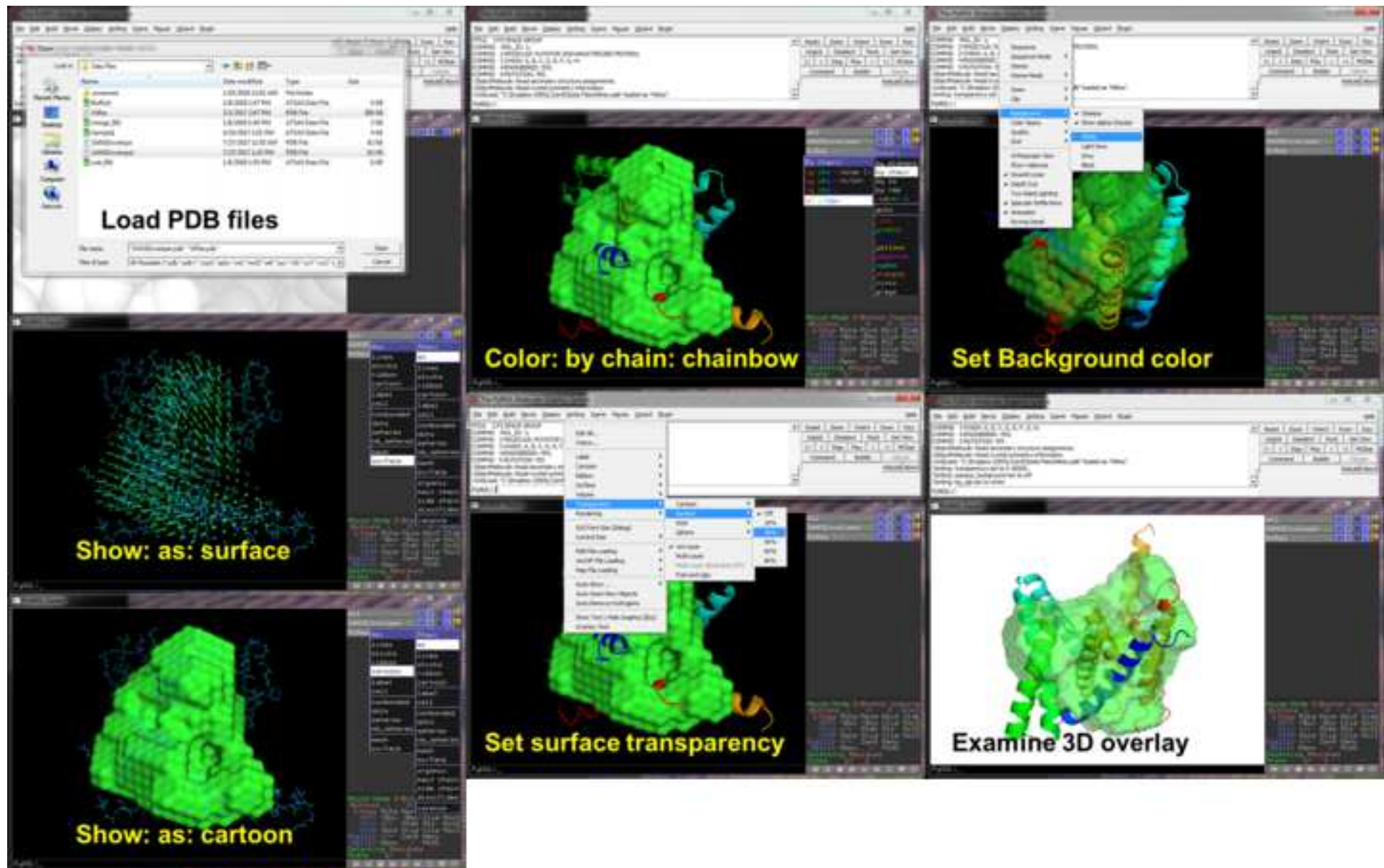
Angular Scale: Angstrom

☒ Average with DAMAVER

☒ Refine with DAMMIN

< Back Commit Cancel

[Click here to download Figure Figure13.tif](#) 



Detergent Name	Common name (abbrev.)	Molecular Formula
n-octyl- β -D-maltopyranoside	Octyl maltoside (OM)	$C_{20}H_{31}X_7O_{11}$
n-decyl- β -D-maltopyranoside	Decyl maltoside (DM)	$C_{22}H_{35}X_7O_{11}$
n-dodecyl- β -D-maltopyranoside	Dodecyl maltoside (DDM)	$C_{24}H_{39}X_7O_{11}$
n-dodecyl-d25-β-D-maltopyranoside	Dodecyl d25-maltoside (d25-DDM)	$C_{24}H_{14}X_7D_{25}O_{11}$
n-decylphosphocholine	Fos-choline 10 (FC10)	$C_{15}H_{34}NO_4P$
n-dodecylphosphocholine	Fos-choline 12 (FC12)	$C_{17}H_{38}NO_4P$
n-tetradecylphosphocholine	Fos-choline 14 (FC14)	$C_{19}H_{42}NO_4P$
n-octyl- β -D-glucopyranoside	Octyl glucoside (OG)	$C_{14}H_{24}X_4O_6$
n-octyl-d17-β-D-glucopyranoside	Octyl d17-glucoside (d17-OG)	$C_{14}D_{17}H_7X_4O_6$
n-octyl-d17-β-D-glucopyranoside-d7	Octyl d24-glucoside (d24-OG)	$C_{14}D_{24}X_4O_6$
n-nonyl- β -D-glucopyranoside	Nonyl glucoside (NG)	$C_{15}H_{26}X_4O_6$
n-decyl- β -D-glucopyranoside	Decyl glucoside (DG)	$C_{16}H_{28}X_4O_6$

*Total volumes are derived from published specific densities, using the Tanford formula ($V_{tail} = 24.7 + 26.7n$), where 'n' is the number of carbons in the hydrophobic tail. 'X' in molecular formulae represents solvent-exchangeable hydrogens. Rows in bold denote deuterium-substituted detergents. ¹CMP is short for 'Contrast Match Point', which is the percentage of D₂O in a D₂O/H₂O mixture at which the scattering contrast is zero.

Head group formula	Tail formula	Formula Weight (g* mol^{-1})	Volume (\AA^3)	Head Group Volume (\AA^3)
$\text{C}_{12}\text{H}_{14}\text{X}_7\text{O}_{11}$	C_8H_{17}	454	590	350
$\text{C}_{12}\text{H}_{14}\text{X}_7\text{O}_{11}$	$\text{C}_{10}\text{H}_{21}$	483	644	350
$\text{C}_{12}\text{H}_{14}\text{X}_7\text{O}_{11}$	$\text{C}_{12}\text{H}_{25}$	511	698	350
$\text{C}_{12}\text{H}_{14}\text{X}_7\text{O}_{11}$	$\text{C}_{12}\text{D}_{25}$	536	698	350
$\text{C}_5\text{H}_{13}\text{NO}_4\text{P}$	$\text{C}_{10}\text{H}_{21}$	323	494	200
$\text{C}_5\text{H}_{13}\text{NO}_4\text{P}$	$\text{C}_{12}\text{H}_{25}$	351	548	200
$\text{C}_5\text{H}_{13}\text{NO}_4\text{P}$	$\text{C}_{14}\text{H}_{29}$	380	602	201
$\text{C}_6\text{H}_7\text{X}_4\text{O}_6$	C_8H_{17}	292	419	179
$\text{C}_6\text{H}_7\text{X}_4\text{O}_6$	C_8D_{17}	310	419	179
$\text{C}_6\text{D}_7\text{X}_4\text{O}_6$	C_8D_{17}	317	419	179
$\text{C}_6\text{H}_7\text{X}_4\text{O}_6$	C_9H_{19}	306	446	179
$\text{C}_6\text{H}_7\text{X}_4\text{O}_6$	$\text{C}_{10}\text{H}_{21}$	320	472	178

5.9*Nc) for alkyl chain volumes to adjust for different chain lengths.

substituted detergents.

the respective 'contrast matched' molecule or moiety becomes invisible to neutron scattering

Alkyl Chain Volume (Å ³)	CMP ¹ -total (%D ₂ O)	CMP-head (%D ₂ O)	CMP-tail (%D ₂ O)
240	26	49	2
294	24	49	2
348	22	49	2
348	84	49	110
294	11	24	2
348	10	24	2
401	10	24	2
240	19	51	2
240	89	51	108
240	118	137	108
267	18	51	2
294	17	52	2

ng

Name	Company
Amicon Ultra MWCO 50KDa concentrator	EMD Millipore
Ammonium citrate dibasic	Fisher Scientific
Ammonium sulfate	EMD Millipore
Bioflo 310 Bioreactor System	Eppendorf
Calcium chloride dihydrate	Acros
Carbenicillin	IBI Scientific
Chloramphenicol	EMD Millipore
Cobalt (II) chloride	Acros
Copper (II) sulfate	Acros
Deuterium oxide	Sigma-Aldrich
Drierite Gas Purifier	W.A. Hammond Drierite Co. Ltd.
EDTA, disodium, dihydrate	EMD Millipore
Emulsiflex-C3	Avestin
Äkta Purifier UPC100	GE Healthcare
Glycerol	Sigma-Aldrich
HEPES	Sigma-Aldrich
HiPrep 16/60 Sephacryl S-300 HR column	GE Healthcare
Imidazole	VWR
IPTG	Teknova
Iron(III) chloride hexahydrate	MP Biochemicals
LB Agar Miller	Fisher Scientific
Magnesium sulfate heptahydrate	VWR
Manganese(II) sulfate monohydrate	Acros
MaxQ 6000 Incubated/Refrigerated Shaker	Thermo Scientific
n-Dodecyl-d25-β-D-maltopyranoside	Anatrace
n-Dodecyl-β-D-maltopyranoside	Anatrace
Potassium phosphate monobasic	VWR
RC 6 Plus Centrifuge	Thermo Scientific Sorvall
SIGMAFAST protease inhibitor cocktail tablets, EDTA-free	Sigma-Aldrich
Sodium chloride	Sigma-Aldrich
Sodium hydroxide	Sigma-Aldrich
Sodium phosphate dibasic	Sigma-Aldrich
Sterile 25mm syringe filter with 0.2µm PES membrane	VWR
Sterile disposable bottle top filter with 0.2µm PES membrane	Thermo Scientific
Superdex 200 10/300 GL	GE Healthcare
Superose-12 10/300 GL column	GE Healthcare
Ultrospec 10 Cell Density Meter	GE Healthcare
Zinc sulfate monohydrate	Acros

Catalog Number	Comments
UFC905096	labware
A663	medium component
2150	medium component
M1287-2110	equipment
423525000	medium component
IB02025	antibiotic
3130	antibiotic
AC21413-0050	medium component
AC19771-1000	medium component
756822	medium component
27068	
4010	medium component
EF-C3	equipment
	equipment
G5516	medium component
H4034	
17116701	
97064-622	
I3325	
ICN19404590	medium component
BP1425-2	
97062-134	medium component
AC20590-5000	medium component
SHKE6000-7	equipment
D310T	
D310A	
97062-346	medium component
46910	equipment
S8830	
S3014	
795429	
S7907	medium component
28145-501	labware
596-4520	labware
17517501	
17517301	
80211630	equipment
AC38980-2500	medium component



1 Alewife Center #200
 Cambridge, MA 02140
 tel. 617.945.9051
 www.jove.com

ARTICLE AND VIDEO LICENSE AGREEMENT

Title of Article: Contrast-Matching Contributions from Detergent in Small-Angle Neutron Scattering Experiments for Membrane Protein Structural Analysis and *Ab Initio* Modeling

Author(s): Volker S. Urban

Item 1 (check one box): The Author elects to have the Materials be made available (as described at <http://www.jove.com/author>) via: ☒ Standard Access ☐ Open Access

Item 2 (check one box):

- ☒ The Author is NOT a United States government employee.
- ☐ The Author is a United States government employee and the Materials were prepared in the course of his or her duties as a United States government employee.
- ☐ The Author is a United States government employee but the Materials were NOT prepared in the course of his or her duties as a United States government employee.

ARTICLE AND VIDEO LICENSE AGREEMENT

1. **Defined Terms.** As used in this Article and Video License Agreement, the following terms shall have the following meanings: “**Agreement**” means this Article and Video License Agreement; “**Article**” means the article specified on the last page of this Agreement, including any associated materials such as texts, figures, tables, artwork, abstracts, or summaries contained therein; “**Author**” means the author who is a signatory to this Agreement; “**Collective Work**” means a work, such as a periodical issue, anthology or encyclopedia, in which the Materials in their entirety in unmodified form, along with a number of other contributions, constituting separate and independent works in themselves, are assembled into a collective whole; “**CRC License**” means the Creative Commons Attribution-Non Commercial-No Derivs 3.0 Unported Agreement, the terms and conditions of which can be found at: <http://creativecommons.org/licenses/by-nc-nd/3.0/legalcode>; “**Derivative Work**” means a work based upon the Materials or upon the Materials and other pre-existing works, such as a translation, musical arrangement, dramatization, fictionalization, motion picture version, sound recording, art reproduction, abridgment, condensation, or any other form in which the Materials may be recast, transformed, or adapted; “**Institution**” means the institution, listed on the last page of this Agreement, by which the Author was employed at the time of the creation of the Materials; “**JoVE**” means MyJoVE Corporation, a Massachusetts corporation and the publisher of *The Journal of Visualized Experiments*; “**Materials**” means the Article and / or the Video; “**Parties**” means the Author and JoVE; “**Video**” means any video(s) made by the Author, alone or in conjunction with any other parties, or by JoVE or its affiliates or agents, individually or in collaboration with the Author or any other parties, incorporating all or any portion of the Article, and in which the Author may or may not appear.

2. **Background.** The Author, who is the author of the Article, in order to ensure the dissemination and protection of the Article, desires to have the JoVE publish the Article and create and transmit videos based on the Article. In furtherance of such goals, the Parties desire to memorialize in this Agreement the respective rights of each Party in and to the Article and the Video.

3. **Grant of Rights in Article.** In consideration of JoVE agreeing to publish the Article, the Author hereby grants to JoVE, subject to **Sections 4 and 7** below, the exclusive, royalty-free, perpetual (for the full term of copyright in the Article, including any extensions thereto) license (a) to publish, reproduce, distribute, display and store the Article in all forms, formats and media whether now known or hereafter developed (including without limitation in print, digital and electronic form) throughout the world, (b) to translate the Article into other languages, create adaptations, summaries or extracts of the Article or other Derivative Works (including, without limitation, the Video) or Collective Works based on all or any portion of the Article and exercise all of the rights set forth in (a) above in such translations, adaptations, summaries, extracts, Derivative Works or Collective Works and (c) to license others to do any or all of the above. The foregoing rights may be exercised in all media and formats, whether now known or hereafter devised, and include the right to make such modifications as are technically necessary to exercise the rights in other media and formats. If the “Open Access” box has been checked in **Item 1** above, JoVE and the Author hereby grant to the public all such rights in the Article as provided in, but subject to all limitations and requirements set forth in, the CRC License.

ARTICLE AND VIDEO LICENSE AGREEMENT

4. Retention of Rights in Article. Notwithstanding the exclusive license granted to JoVE in Section 3 above, the Author shall, with respect to the Article, retain the non-exclusive right to use all or part of the Article for the non-commercial purpose of giving lectures, presentations or teaching classes, and to post a copy of the Article on the Institution's website or the Author's personal website, in each case provided that a link to the Article on the JoVE website is provided and notice of JoVE's copyright in the Article is included. All non-copyright intellectual property rights in and to the Article, such as patent rights, shall remain with the Author.

5. Grant of Rights in Video – Standard Access. This Section 5 applies if the "Standard Access" box has been checked in Item 1 above or if no box has been checked in Item 1 above. In consideration of JoVE agreeing to produce, display or otherwise assist with the Video, the Author hereby acknowledges and agrees that, Subject to Section 7 below, JoVE is and shall be the sole and exclusive owner of all rights of any nature, including, without limitation, all copyrights, in and to the Video. To the extent that, by law, the Author is deemed, now or at any time in the future, to have any rights of any nature in or to the Video, the Author hereby disclaims all such rights and transfers all such rights to JoVE.

6. Grant of Rights in Video – Open Access. This Section 6 applies only if the "Open Access" box has been checked in Item 1 above. In consideration of JoVE agreeing to produce, display or otherwise assist with the Video, the Author hereby grants to JoVE, subject to Section 7 below, the exclusive, royalty-free, perpetual (for the full term of copyright in the Article, including any extensions thereto) license (a) to publish, reproduce, distribute, display and store the Video in all forms, formats and media whether now known or hereafter developed (including without limitation in print, digital and electronic form) throughout the world, (b) to translate the Video into other languages, create adaptations, summaries or extracts of the Video or other Derivative Works or Collective Works based on all or any portion of the Video and exercise all of the rights set forth in (a) above in such translations, adaptations, summaries, extracts, Derivative Works or Collective Works and (c) to license others to do any or all of the above. The foregoing rights may be exercised in all media and formats, whether now known or hereafter devised, and include the right to make such modifications as are technically necessary to exercise the rights in other media and formats. For any Video to which this Section 6 is applicable, JoVE and the Author hereby grant to the public all such rights in the Video as provided in, but subject to all limitations and requirements set forth in, the CRC License.

7. Government Employees. If the Author is a United States government employee and the Article was prepared in the course of his or her duties as a United States government employee, as indicated in Item 2 above, and any of the licenses or grants granted by the Author hereunder exceed the scope of the 17 U.S.C. 403, then the rights granted hereunder shall be limited to the maximum rights permitted under such

statute. In such case, all provisions contained herein that are not in conflict with such statute shall remain in full force and effect, and all provisions contained herein that do so conflict shall be deemed to be amended so as to provide to JoVE the maximum rights permissible within such statute.

8. Likeness, Privacy, Personality. The Author hereby grants JoVE the right to use the Author's name, voice, likeness, picture, photograph, image, biography and performance in any way, commercial or otherwise, in connection with the Materials and the sale, promotion and distribution thereof. The Author hereby waives any and all rights he or she may have, relating to his or her appearance in the Video or otherwise relating to the Materials, under all applicable privacy, likeness, personality or similar laws.

9. Author Warranties. The Author represents and warrants that the Article is original, that it has not been published, that the copyright interest is owned by the Author (or, if more than one author is listed at the beginning of this Agreement, by such authors collectively) and has not been assigned, licensed, or otherwise transferred to any other party. The Author represents and warrants that the author(s) listed at the top of this Agreement are the only authors of the Materials. If more than one author is listed at the top of this Agreement and if any such author has not entered into a separate Article and Video License Agreement with JoVE relating to the Materials, the Author represents and warrants that the Author has been authorized by each of the other such authors to execute this Agreement on his or her behalf and to bind him or her with respect to the terms of this Agreement as if each of them had been a party hereto as an Author. The Author warrants that the use, reproduction, distribution, public or private performance or display, and/or modification of all or any portion of the Materials does not and will not violate, infringe and/or misappropriate the patent, trademark, intellectual property or other rights of any third party. The Author represents and warrants that it has and will continue to comply with all government, institutional and other regulations, including, without limitation all institutional, laboratory, hospital, ethical, human and animal treatment, privacy, and all other rules, regulations, laws, procedures or guidelines, applicable to the Materials, and that all research involving human and animal subjects has been approved by the Author's relevant institutional review board.

10. JoVE Discretion. If the Author requests the assistance of JoVE in producing the Video in the Author's facility, the Author shall ensure that the presence of JoVE employees, agents or independent contractors is in accordance with the relevant regulations of the Author's institution. If more than one author is listed at the beginning of this Agreement, JoVE may, in its sole discretion, elect not take any action with respect to the Article until such time as it has received complete, executed Article and Video License Agreements from each such author. JoVE reserves the right, in its absolute and sole discretion and without giving any reason therefore, to accept or decline any work submitted to JoVE. JoVE and its employees, agents and independent contractors shall have

ARTICLE AND VIDEO LICENSE AGREEMENT

full, unfettered access to the facilities of the Author or of the Author's institution as necessary to make the Video, whether actually published or not. JoVE has sole discretion as to the method of making and publishing the Materials, including, without limitation, to all decisions regarding editing, lighting, filming, timing of publication, if any, length, quality, content and the like.

11. **Indemnification.** The Author agrees to indemnify JoVE and/or its successors and assigns from and against any and all claims, costs, and expenses, including attorney's fees, arising out of any breach of any warranty or other representations contained herein. The Author further agrees to indemnify and hold harmless JoVE from and against any and all claims, costs, and expenses, including attorney's fees, resulting from the breach by the Author of any representation or warranty contained herein or from allegations or instances of violation of intellectual property rights, damage to the Author's or the Author's institution's facilities, fraud, libel, defamation, research, equipment, experiments, property damage, personal injury, violations of institutional, laboratory, hospital, ethical, human and animal treatment, privacy or other rules, regulations, laws, procedures or guidelines, liabilities and other losses or damages related in any way to the submission of work to JoVE, making of videos by JoVE, or publication in JoVE or elsewhere by JoVE. The Author shall be responsible for, and shall hold JoVE harmless from, damages caused by lack of sterilization, lack of cleanliness or by contamination due to the making of a video by JoVE its employees, agents or independent contractors. All sterilization, cleanliness or decontamination procedures shall be solely the responsibility of the Author and shall be undertaken at the Author's

expense. All indemnifications provided herein shall include JoVE's attorney's fees and costs related to said losses or damages. Such indemnification and holding harmless shall include such losses or damages incurred by, or in connection with, acts or omissions of JoVE, its employees, agents or independent contractors.

12. **Fees.** To cover the cost incurred for publication, JoVE must receive payment before production and publication the Materials. Payment is due in 21 days of invoice. Should the Materials not be published due to an editorial or production decision, these funds will be returned to the Author. Withdrawal by the Author of any submitted Materials after final peer review approval will result in a US\$1,200 fee to cover pre-production expenses incurred by JoVE. If payment is not received by the completion of filming, production and publication of the Materials will be suspended until payment is received.

13. **Transfer, Governing Law.** This Agreement may be assigned by JoVE and shall inure to the benefits of any of JoVE's successors and assignees. This Agreement shall be governed and construed by the internal laws of the Commonwealth of Massachusetts without giving effect to any conflict of law provision thereunder. This Agreement may be executed in counterparts, each of which shall be deemed an original, but all of which together shall be deemed to me one and the same agreement. A signed copy of this Agreement delivered by facsimile, e-mail or other means of electronic transmission shall be deemed to have the same legal effect as delivery of an original signed copy of this Agreement.

A signed copy of this document must be sent with all new submissions. Only one Agreement required per submission.

CORRESPONDING AUTHOR:

Name:

Department:

Institution:

Article Title:

Signature: Date:

Please submit a signed and dated copy of this license by one of the following three methods:

- 1) Upload a scanned copy of the document as a pdf on the JoVE submission site;
- 2) Fax the document to +1.866.381.2236;
- 3) Mail the document to JoVE / Attn: JoVE Editorial / 1 Alewife Center #200 / Cambridge, MA 02139

For questions, please email submissions@jove.com or call +1.617.945.9051

1. The highlighted portion is too long (currently roughly between 3.5 and 4 pages; note that headers should also be highlighted (e.g., if 1.1.1 is highlighted, 1.1 and 1 should be highlighted as well)) and somewhat sketchy and lacking in detail in places. Generally, this can be improved by selecting only certain sections to be filmed; as is, some portions of the current protocol seem more vague/harder to film or are somewhat less essential to be filmed (common techniques or guided by expert help during the protocol itself), like 1 and much of 3 and 4.

[We have thoroughly revised highlighting following the review comments. Highlighted sections are now well below the 2.75 page limit. We have also drafted notes with our suggestions for filming specific segments. These are included at the end of this document.](#)

2. Figure 4 is reproduced from another paper; please include explicit copyright permission in the form of a letter from the editor or a link to the editorial policy that allows re-prints. Please upload this information as a .doc or .docx file to your Editorial Manager account.

[We have obtained permission and are including a document that confirms this with our resubmission.](#)

3. Figure 4 still has 'mI' instead of 'mL'; please fix this.

[This has been fixed. I apologize for the oversight of not including an updated Figure 4 with our previous submission.](#)

4. Please include websites as cited references rather than including the URL in the text.

[This has been done in the new version.](#)

Addendum: Suggestions for filming specific segments

We would like to suggest organization of the video into 4 general 'scenes', which might appear in somewhat of a different order than the text, if this is acceptable:

- 1) Protein/sample preparation demonstration taking place in the bio-deuteration lab facility [live action],
- 2) Information on how to select the appropriate buffer conditions and calculate contrast using appropriate software [video/software tutorial],
- 3) Sample loading on the instrument and setup for data collection at the Bio-SANS instrument [live action], and
- 4) Data analysis and interpretation from the collected data [video/software tutorial].

From: Permissions Helpdesk <permissionshelpdesk@elsevier.com>
Sent: Thursday, April 12, 2018 2:25 PM
To: Lieberman, Raquel L <raquel.lieberman@chemistry.gatech.edu>
Cc: Urban, Volker S. <urbanvs@ornl.gov>
Subject: RE: Thank you for your order with RightsLink / Elsevier

Dear Dr. Liberman,

Yes, it looks like permission was granted to you free of charge. No further action is required.

Best Wishes,
Laura

Laura Stingelin
Permissions Helpdesk
ELSEVIER | Global E-Operations Books
+1 215-239-3867 office
l.stingelin@elsevier.com
Contact the Permissions Helpdesk
permissionshelpdesk@elsevier.com

From: Lieberman, Raquel L [<mailto:raquel.lieberman@chemistry.gatech.edu>]
Sent: Wednesday, April 11, 2018 3:22 PM
To: Permissions Helpdesk <permissionshelpdesk@elsevier.com>
Cc: Urban, Volker S. <urbanvs@ornl.gov>
Subject: Fwd: Thank you for your order with RightsLink / Elsevier

***** External email: use caution *****

Hi,
I am attempting to get copyright clearance to use a figure from one of my papers in another. I got this email when I went through the copyright clearance center, and this link <https://s100.copyright.com/CustomerAdmin/PLF.jsp?ref=2e8c0fb8-22d7-4820-a747-96c4c2a5d9da> . Is this all I need for official permission?

Thank you for your assistance,
Raquel

Raquel L. Lieberman, Ph.D.
Associate Professor
School of Chemistry and Biochemistry
Georgia Institute of Technology
901 Atlantic Drive, NW
Atlanta, GA 30332-0400
e-mail: raquel.lieberman@chemistry.gatech.edu

Phone: (404) 385-3663

website: <http://www.chemistry.gatech.edu/people/lieberman/raquel>

Begin forwarded message:

From: <no-reply@copyright.com>

Subject: Thank you for your order with RightsLink / Elsevier

Date: April 4, 2018 at 7:45:39 PM EDT

To: <raquel.lieberman@chemistry.gatech.edu>

<image001.jpg>

Thank you for your order!

Dear Prof. Raquel Lieberman,
Thank you for placing your order through Copyright Clearance Center's RightsLink® service.

Order Summary

Licensee: Georgia Institute of Technology
Order Date: Apr 4, 2018
Order Number: 4322180721585
Publication: Biophysical Journal
Title: Solution Structure of an Intramembrane Aspartyl Protease via Small Angle Neutron Scattering
Type of Use: reuse in a journal/magazine
Order Total: 0.00 USD

View or print complete [details](#) of your order and the publisher's terms and conditions.

Sincerely,

Copyright Clearance Center

How was your experience? Fill out this [survey](#) to let us know.

Tel: +1-855-239-3415 / +1-978-646-2777

customercare@copyright.com

<https://myaccount.copyright.com>

==



Thank you for your order!

Dear Prof. Raquel Lieberman,

Thank you for placing your order through Copyright Clearance Center's RightsLink® service.

Order Summary

Licensee: Georgia Institute of Technology
Order Date: Apr 4, 2018
Order Number: 4322180721585
Publication: Biophysical Journal
Title: Solution Structure of an Intramembrane Aspartyl Protease via Small Angle Neutron Scattering
Type of Use: reuse in a journal/magazine
Order Total: 0.00 USD

View or print complete [details](#) of your order and the publisher's terms and conditions.

Sincerely,

Copyright Clearance Center

How was your experience? Fill out this [survey](#) to let us know.

Tel: +1-855-239-3415 / +1-978-646-2777
customer care@copyright.com
<https://myaccount.copyright.com>



RightsLink®